Mol Divers (2014) 18:577–592
DOI 10.1007/s11030-014-9528-4

FULL-LENGTH PAPER

# Antiproliferative activity of the Michael adducts of aroylacrylic acids and cyclic amines

**Ivan O. Juranić · Ana V. Tošić · Branka Kolundžija · Branko J. Drakulić**

Received: 19 December 2013 / Accepted: 6 May 2014 / Published online: 30 May 2014


**Abstract** Antiproliferative activity of twenty one Michael adducts of aroylacrylic acids and cyclic amines (*N*-Me-piperazine, imidazole, 2-Me-imidazole, and indole) was tested toward five human tumor cell lines (HeLa, LS174, K562, FemX, MDA-MB-361) in vitro. Compounds exerted antiproliferative activity in the high to the single-digit micromolar concentrations, causing increase of the cell population fraction in S phase and apoptosis. *N*-Me-piperazine and imidazole derivatives of aroylacrylic acids substituted with bulky alkyl substituents (2,4-di-*i*-Pr-Ph-, 2,4,6-tri-Et-Ph-, or $\beta$-tetrahydronaphthyl-) showed the best potency, while indole adducts were proved as the inferior antiproliferative agents. Few compounds showed significant selectivity, tumor versus healthy cells, with selectivity index ∼60 for the most selective congener. An unbiased in silico distinction between more and less potent compounds was obtained from 3D QSAR models derived by alignment-independent GRIND-2 descriptors.

**Keywords** Antiproliferative activity · Selectivity · Michael adducts · Aroylacrylic acids · 3D QSAR

**Electronic supplementary material** The online version of this article (doi:10.1007/s11030-014-9528-4) contains supplementary material, which is available to authorized users.

I. O. Juranić · B. J. Drakulić (✉)
Department of Chemistry – IChTM, University of Belgrade, Njegoševa 12, 11000 Belgrade, Serbia
e-mail: bdrakuli@chem.bg.ac.rs

A. V. Tošić
Laboratory for Conservation and Restoration, National Archive of Serbia, Karnegijeva 2, 11000 Belgrade, Serbia

B. J. Kolundžija
Institute for Oncology and Radiology, Pasterova 14, 11000 Belgrade, Serbia

## Introduction

Although additions of amines to aroylacrylic acids have been initially described in [1], and the regioselectivity of the reaction was evaluated in more detail in [2], there are just few literature data on Michael adducts of aroylacrylic acids and cyclic amines that exert biological activity. Such compounds are reported as inhibitors of the 1,4-dihydroxy-2-naphthoyl-CoA synthase from the menaquinone biosynthesis pathway in *Mycobacterium tuberculosis* [3] and as an auxin antagonist of the $SCF^{TIR1}$ auxin receptor complex [4]. A Michael adduct of morpholine and benzoylacrylic acid (PubChem CID 288825) has been found active in a NCI yeast screen, but inactive against all of the NCI 60-cell lines. The same derivative inhibits HePTP, tyrosine-protein phosphatase non-receptor type 7, isoform 2, as revealed from data obtained by high-throughput screening (AID 376) [5] deposited in PubChem database [6]. Along with this, antibacterial activity of the Michael adducts of morpholine with 4-F-Ph-, 4-Cl-Ph-, 4-$NO_2$-Ph-, and 4-MeO-Ph- benzoylacrylic acids has been reported [7], while cytostatic activity toward human lymphocytes stimulated for growth was reported for Michael adducts of piperidine and 4-(hydroxyethyl)piperazine with 4-Cl-Ph-benzoylacrylic acid [8].

## Results and discussion

Herein we report antiproliferative activities of twenty one Michael adducts of aroylacrylic acids and cyclic amines (*N*-Me-piperazine, imidazole, 2-Me-imidazole, and indole) toward human tumor cell lines in vitro. Aroylacrylic acids, their *S*-Michael adducts with thioglycolic acid, and amides exert antiproliferative activity in vitro [9–11]. In each congeneric set prepared so far, compounds having bulky alkyl

substituents on the aroyl moiety have been found to be the most active. For this reason, we used aroylacrylic acids with mainly hydrophobic substituents as synthetic precursors of the title compounds. Precursors (**P1**–**P10**) were prepared by Friedel–Crafts acylation of substituted benzenes with maleic acid anhydride in $CH_2Cl_2$, using $AlCl_3$ as a catalyst (Scheme 1) in high yields [9,12]. Target compounds were obtained by mixing aroylacrylic acid with ∼1.2 molar equivalents of cyclic amine in the mixture of $CH_2Cl_2$/toluene at room temperature (Scheme 1; Table 1). Products were separated by filtration. For details, see "Experimental" part. All target compounds (**1**–**21**) were isolated as the mixture of *R* and *S* enantiomers, and used as such for biological tests. The stereogenic center in all compounds is situated in position 2 of the butanoic moiety of compounds.

Some of the prepared compounds were insoluble in both DMSO and water (**1**, **5**, **8**–**12**, Table 1). Solubility in one of those solvents is a requisite for biological tests. Such compounds were converted to sodium salts. Both neutral species and corresponding sodium salts were characterized by instrumental techniques. Along with this, we prepared a few congeners that were insoluble in DMSO, $CHCl_3$, MeOH, and water (see Supplementary material, Fig. S1). These derivatives showed one spot on TLC plate after purification, and were characterized by meting points and IR spectroscopy only. Every attempt of conversion to sodium salts caused decomposition of these compounds. It is obvious that both the substitution pattern of the aroyl part of molecule and the nature of the Michael donor strongly influence stability, solubility, and synthetic feasibility of the compounds, although

**Table 1** Structure of compounds **1**–**21**

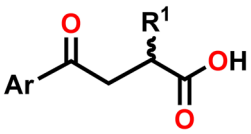


| Compound no | Ar | $R^1$ |
|---|---|---|
| **1a*** | 4-*tert*-Bu-Ph | 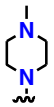 |
| **2** | 2,5-di-Me-Ph | |
| **3** | 2,4-di-*i*-Pr-Ph | |
| **4** | *β*-tetralinyl | |
| **5a** | 2,5-di-Me-Ph |  |
| **6** | 2,4-di-*i*-Pr-Ph | |
| **7a** | *β*-tetralinyl | |
| **8a** | 2,4,6-tri-Et-Ph | |
| **9a** | 4-*tert*-Bu-Ph |  |
| **10a** | 3,4-di-Me-Ph | |
| **11a** | *β*-tetralinyl | |
| **12a** | 2,4,6-tri-Et-Ph | |
| **13** | 4-F-Ph | 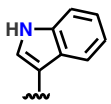 |
| **14** | 4-Et-Ph | |
| **15** | 4-*i*-Pr-Ph | |
| **16** | 4-*tert*-Bu-Ph | |
| **17** | 2,4-di-Me-Ph | |
| **18** | 2,5-di-Me-Ph | |
| **19** | 3,4-di-Me-Ph | |
| **20** | 2,4-di-*i*-Pr-Ph | |
| **21** | 2,4,6-tri-Et-Ph | |

* Compounds tested as the sodium salts are marked with **a**

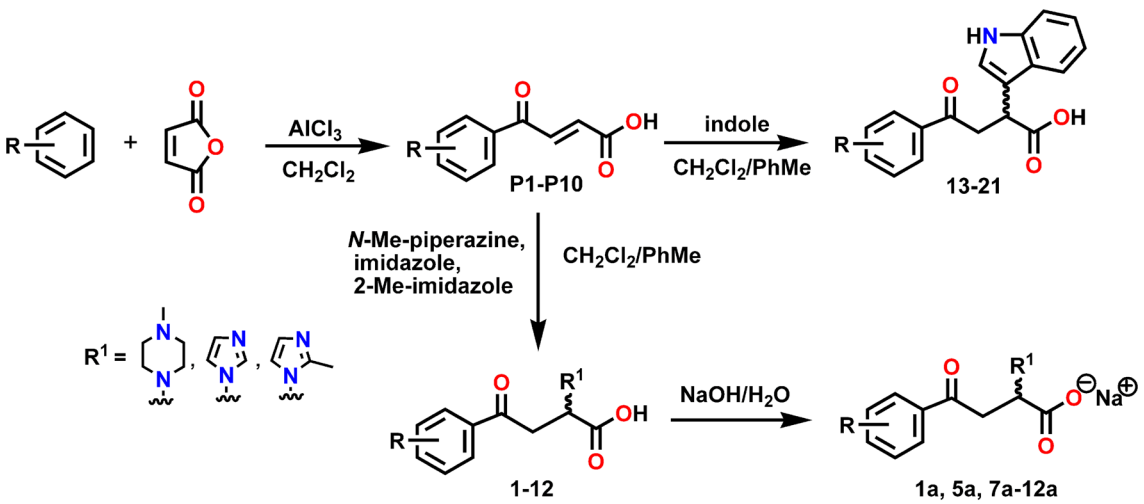


**R-** = 4-Et, 4-*i*-Pr, 4-*tert*-Bu, 2,4-di-Me, 3,4-di-Me, 2,5-di-Me, *β*-tetralinyl, 2,4-di-*i*-Pr, 2,4,6-tri-Et, 4-F.

**Scheme 1** Synthesis of compounds **1**–**21**

**Table 2** Cytotoxicity of compounds **1**–**21** toward human tumor cell lines

| $IC_{50}$± SD (μM) | | | | | |
|---|---|---|---|---|---|
| Compound | HeLa | LS174 | K562 | FemX | MDA-MB-361 |
| **1a** | 6.70 ± 1.67 | 12.92 ± 1.29 | 4.22 ± 1.29 | 11.27± 0.30 | 17.22 ± 2.39 |
| **2** | 10.23 ± 1.49 | 16.29 ± 3.28 | 4.35 ± 0.40 | 9.53 ±0.13 | 18.45 ± 1.84 |
| **3** | 3.54 ± 1.01 | 4.63 ± 1.08 | 0.95 ± 0.12 | 4.70 ±0.94 | 6.99 ± 0.65 |
| **4** | 5.86 ± 0.18 | 14.03 ± 1.39 | 4.63 ± 1.45 | 8.86 ± 1.00 | 13.81 ± 1.35 |
| **5a** | 20.08 ± 0.87 | ~55.00 | 16.45 ± 1.42 | 30.25 ± 4.42 | 39.32 ± 2.05 |
| **6** | 3.29 ± 0.48 | 5.15 ± 1.33 | 1.15 ± 0.25 | 4.67 ± 0.60 | 6.92 ± 0.72 |
| **7a** | 21.10 ± 2.65 | 62.58 ± 9.09 | 12.21 ± 0.66 | 31.66 ± 0.70 | 39.07 ± 2.91 |
| **8a** | 11.16 ± 2.26 | 13.04 ± 2.04 | 1.50 ± 0.43 | 11.24 ± 1.34 | 12.10 ± 0.49 |
| **9a** | 14.49 ± 3.09 | 38.19 ± 8.06 | 9.67 ± 0.75 | 20.30 ± 2.83 | 31.39 ± 5.54 |
| **10a** | >200 | >200 | >200 | >200 | >200 |
| **11a** | 27.03 ± 8.22 | 84.66 ± 10.49 | 15.36 ± 1.26 | 35.23 ± 4.42 | 45.20 ± 3.67 |
| **12a** | 5.94 ± 2.65 | 8.43 ± 2.30 | 1.20 ± 0.34 | 7.71 ± 1.97 | 8.18 ± 0.73 |
| **13** | 107.85 ± 4.29 | 146.10 ± 0.93 | 62.51 ± 11.07 | ND | ND |
| **14** | 93.89 ± 11.45 | ND | ND | 100.00 ± 0.05 | 97.76 ± 3.16 |
| **15** | 67.52 ± 18.13 | ND | 33.12 ± 6.35 | 82.75 ± 4.14 | 80.97 ± 5.23 |
| **16** | 50.56 ± 12.45 | ND | 34.16 ± 9.10 | 54.35 ± 7.14 | 54.26 ± 9.05 |
| **17** | 65.23 ± 9.15 | ND | 50.50 ± 13.45 | 94.54 ± 2.48 | ND |
| **18** | 80.25 ± 5.16 | 122.76 ± 8.04 | 47.57 ± 0.41 | 119.28 ± 6.87 | 108.30 ±1.03 |
| **19** | 83.76 ± 10.40 | ND | 45.91 ± 11.51 | 100.00 ± 0.05 | 98.45 ± 2.19 |
| **20** | 64.70 ± 1.14 | 76.17 ± 2.18 | 28.51 ± 4.92 | 67.11 ± 4.58 | ND |
| **21** | 49.29 ± 5.72 | 62.11 ± 1.35 | 23.87 ± 2.49 | 59.33 ± 3.54 | 76.57 ± 7.41 |
| Cisplatin | 6.05 ± 0.70 | 13.48 ± 5.21 | 3.64 ± 1.38 | 11.40 ± 3.50 | 31.71 ± 1.63 |

*ND*–not determined

we dealt with a relatively small set of congeneric compounds. For example, compound **20**, *C*-adduct of indole and (*E*)-(2,4-di-*i*-Pr-Ph)-4-oxo-2-butenoic acid (**P8**), has been obtained in a fair yield only after three days of mixing of reagents at room temperature and subsequent recrystallization. We were unable to obtain the Michael adduct of indole and (*E*)-4-(5,6,7,8-tetrahydronaphthalene-2-yl)-4-oxo-2-butenoic acid (**P7**) in recognizable yield (Supplementary material, Fig. S1). Published procedures for synthesis of the addition products of indole and 4-(anthracen-9-yl)-4-oxo-2-butenoic acid, or of 4-(2,5-di-Me-Ph)-4-oxo-2-butenoic acid and 4-(biphenyl-4-yl-)-4-oxo-2-butenoic acid (structurally similar or identical to **P1**–**P8**), reporting that the product was obtained by refluxing of reagents in dry benzene [13,14], turned out to be irreproducible in our hands.

Michael addition of *N*-Me-piperazine, imidazole, and 2-Me-imidazole provided *N*-addition products, while *C*-addition products were obtained in reaction with indole. Addition of all donors proceeded exclusively in $\beta$-position with respect to the aroyl keto group of aroylacrylic acids. Regioselectivity of additions was confirmed by instrumental techniques and is in accordance with the literature data. The section of the NOESY spectrum that shows spatial vicinity of AB protons of the ABX pattern with the *ortho*-hydrogen of the aroyl moiety for derivative **6** is given in Fig. S2 in Supplementary material, as an example.

Antiproliferative potency of compounds **1**–**21** toward five human tumor cell lines (HeLa—human cervix carcinoma, LS174—human colon carcinoma, K562—human myelogenous leukemia, FemX—human malignant melanoma, MDA-MB-361—breast carcinoma) was evaluated by MTT test, after 72 h of exposure of cells to compounds (Table 2). Potency of compounds is expressed as $IC_{50}$ values, a molar concentration which induces 50 % decrease in cell survival. The indole derivatives, which in high concentrations exerted low antiproliferative activity toward the first few cell lines tested, were not evaluated any further in other cell lines.

*N*-Me-piperazine, imidazole, and 2-Me-imidazole derivatives (**1**–**12**) showed significantly better potency toward all cell lines tested, compared to indole adducts. As an exception, compound **10** proved to be inactive. We were unable to test addition products of *N*-Me-piperazine and imidazole on 4-(3,4-di-Me-Ph)-4-oxo-2-butenoic acid (**P5**), due to their insolubility in DMSO, water, and the majority of organic solvents. Attempts to convert those derivatives to salts failed due to decomposition. Therefore, we can suppose that the analo-

**Table 3** Cytotoxicity of compounds **2**–**4**, **6** and **12a** toward healthy cells, non-stimulated (PMBC − PHA), or stimulated for growth (PMBC + PHA); and selectivity indexes ($S_i$)

| Compound | PMBC − PHA, $IC_{50} \pm SD$ (μM) | $S_i$ range |
|---|---|---|
| **2** | 7.66 ± 1.43 | 0.41–1.76 |
| **3** | 56.48 ± 6.77 | 8.08–59.45 |
| **4** | 42.45 ± 19.06 | 3.02–9.17 |
| **6** | 40.17 ± 3.36 | 5.80–34.93 |
| **12a** | 12.91 ± 2.42 | 1.53–10.76 |
| Compound | PMBC + PHA, $IC_{50} \pm SD$ (μM) | $S_i$ range |
| **2** | 6.06 ± 0.19 | 0.33–1.39 |
| **3** | 35.78 ± 14.67 | 5.12–37.66 |
| **4** | 34.77 ± 18.55 | 2.48–7.51 |
| **6** | 29.58 ± 5.51 | 5.74–25.72 |
| **12a** | 11.01 ± 0.94 | 1.31–9.17 |

gous 2-Me-imidazole derivative is insufficiently stable under assay conditions. From this end, it should be noted that parent aroylacrylic acid **P5** showed antiproliferative potency toward K562, HeLa, and LS174 cells with $IC_{50}$ of ~6–12 μM [9], so retro-Michael reaction most probably cannot explain the lack of activity of derivative **10**. Among *N*-addition products, compounds substituted with bulky alkyl substituents on the aroyl phenyl ring showed best potency toward all cell lines tested within each subset (*N*-Me-piperazine, imidazole, or 2-Me-imidazole derivatives). Such trend could not be ascribed to a mere increase of the lipophilicity of compounds within each subset, nor within the whole set (see Table S1 in Supplementary material).

Cytotoxicity of five compounds (**2**, **3**, **4**, **6**, and **12a**) toward healthy human cells non-stimulated or stimulated for growth was also evaluated. Compounds **3**, **6**, and **12a** were chosen as the most potent within each subset of *N*-addition products. We included compounds **2** and **4** to find out whether there is some correlation between potency against tumor cells and cytotoxicity toward healthy cells within one subset. For each examined tumor cell line, the selectivity index was calculated as the ratio between $IC_{50}$ values toward healthy cells and $IC_{50}$ values toward tumor cells. Most potent antiproliferative agents were also among the most selective compounds tested (Table 3).

Healthy human cells stimulated for growth appeared more susceptible toward the action of compounds, comparing with non-stimulated cells. This finding, along with results obtained in cell cycle analysis (for compounds **3**, **6** and **12a**), implies components of pathways that regulate cell proliferation as the possible molecular targets. Given that one of the most prominent characteristics of cancer cells is their uncontrollable proliferation, compounds that target these pathways are very useful in clinical practice.

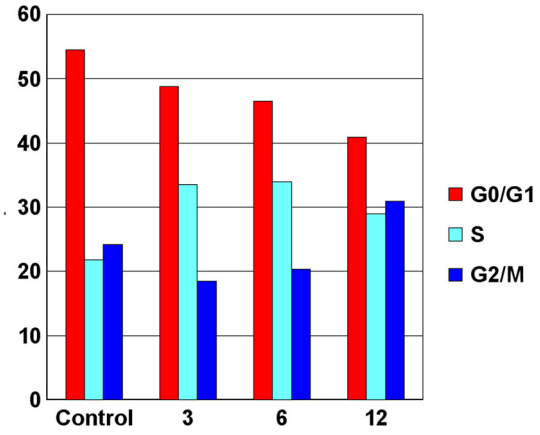


**Fig. 1** Cell cycle analysis of HeLa cells treated with one $IC_{50}$ of compounds **3**, **6**, and **12a**, during 24 h

Compound **3**, the *N*-Me-piperazine adduct of 4-(2,4-di-*i*-Pr-Ph)-4-oxo-2-butenoic acid, appeared as both the most potent and the most selective derivative, being eight to almost sixty times less toxic toward healthy cells when compared with malignant cells. Compounds **6** and **12** also showed good selectivity profile. Compound **4** showed inferior selectivity comparing to compound **3**, while compound **2** appeared almost non-selective, exerting higher toxicity toward healthy cells than toward HeLa, LS174, FemX, and MDA-MB-361 cells.

Cell cycle analysis shows that compounds **3** and **6** cause accumulation of cells in S phase, while compound **12** causes an increase of the number of cells in both S and G2/M phases, compared to the control (Fig. 1; Table S2 in Supplementary material).

The type of cell death was examined by acridine orange/ethidium bromide (AO/EB) staining. Acridine orange is a vital dye that can stain nuclear DNA across an intact cell membrane, whereas ethidium bromide can stain only cells with lost membrane integrity. Fluorescent microscopy of HeLa cells stained with AO/EB after exposure by compounds **2**, **3**, and **4** showed condensed nuclei of cells (Fig. S3 in Supplementary material); *N*-Me-piperazinyl derivatives caused apoptosis in HeLa cells.

To put structure-activity relationships of antiproliferative potency of compounds in tumor cell lines on quantitative ground, we built 3D QSAR models using alignment-independent GRIND-2 descriptors derived from GRID [15, 16] molecular interaction fields (MIF), as applied in Pentacle program [17]. GRIND variables are extracted from MIFs' local minima calculated around examined molecules, using different GRID probes. We used HBD (N1), HBA (O), hydrophobic (DRY), and shape (TIP) probes. Each GRIND descriptor consists of two nodes extracted from MIFs and encodes their energy product and the spatial distance. GRIND variables represent geometrical relationships between relevant pharmacophoric points around stud-

ied molecules. Variables are entirely independent on spatial position of molecule(s) and their alignment. GRIND variables can be used for similarity search among molecules, virtual screening, and 3D QSAR. For more information on the methodology applied, see original reference [18]. Compounds **1**–**9** and **11**–**21** (all congeners with $IC_{50}$ values <200 μM) were submitted to the program and GRIND-2 descriptors were calculated. Principal component analysis (PCA) obtained with five principal components (PC) explained 72 % variance in the set (Table S3 in Supplementary material). Good distinction among subsets of compounds, according to the added Michael donor, was obtained in the space of the first two PC (Fig. S4 in Supplementary material).

For structure-activity relationships study, activity of compounds was imported and 3D QSAR models built for the potency data toward each tested tumor cell line, using partial least square analysis (PLS). Good correlations were obtained with the two or the three latent variables (LV), depending on the cell line examined.

The squared coefficients of determination ($r^2$) obtained were in the range from 0.84 to 0.98; the the cross-validated squared predictive correlation coefficient ($q^2$) was in the range between 0.57 and 0.89, depending on the cell lines for which the model was derived and on the method of the cross-validation (leave-one-out, leave-two-out, or cross-validation performed using four random groups of compounds).

In Table S4 of the Supplementary material, statistics of PLS models are given; in Table S5, experimental *vs*. calculated values, as obtained from models, are listed. PLS coefficient plots are shown in Fig. 2 and in Fig. S5 of the Supplementary material.

Each bar on the plot corresponds to one variable. Intensity of variables corresponds to overall contribution of the particular variable to the potency of compounds. Positive variables describe the combination of two pharmacophoric points and their spatial distance that positively contribute to potency, while negative variables describe pharmacophoric motifs that negatively contribute to potency. PLS coefficient plots appeared mutually very similar, indicating similar pattern of potency of compounds toward the tested tumor cell lines. Both the graphical presentation of the potency of all (tested and active) compounds toward all tumor cell lines and the intercorrelation matrix of $IC_{50}$ values of all compounds toward all tumor cell lines tested, indeed, showed a similar trend of potency (Supplementary material, Table S6; Fig. S6). From those data, we may infer a similar mode of action of the compounds.

Variables in PLS models positively correlated with the potency of compounds outline following pharmacophoric features favorable for potency: (a) Bulky substituents on aroyl phenyl ring on the distance of ∼18 Å of the distal parts of heterocyclic rings attached to C2 of the butanoic moiety (variable TIP-TIP 248); (b) Torsion angle between aroyl phenyl and aroyl keto group. Voluminous substituents in *ortho*-position of the aroyl phenyl ring cause a significant torsion around Ar–C(O). Such compounds are more potent comparing to the rest. In this way, the aroyl carbonyl oxygen, as a HBA, is more exposed to surroundings, compared to the rest of compounds (variable DRY-N1 324); (c) Distance of about 5 Å between aroyl carbonyl group, as HBA, and protonated piperazino N4, as HBD. This variable is specific for

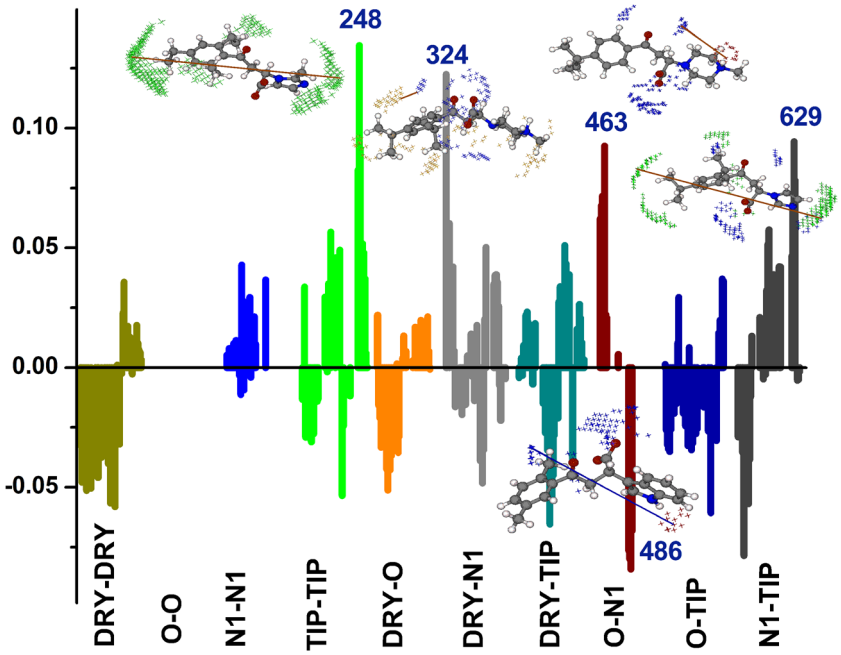


**Fig. 2** 3LV PLS coefficients plot for the model of antiproliferative activity of compounds **1**–**9**, **11**–**21** toward HeLa cells. Most important variables are marked and illustrated

*N*-Me-piperazinyl derivatives (variable O-N1 463); (d) Distance of ∼17 Å between aroyl substituents in position 4 and HBA (N3 of imidazolo moiety) in the imidazolyl derivatives (variable N1-TIP 629).

Along with this, distance of about 12 Å between HBD, NH group of indolyl moiety, and HBA-aroyl keto group is recognized as the pharamacophoric pattern negatively correlated with the potency of compounds (variable O-N1 486, expressed for all indolyl derivatives). All above-described variables are illustrated on Fig. 2 and on Fig. S7 in the Supplementary material. A more stringent interpretation of variables, on the example of the HeLa model, is given in the Supplementary material, as well as the association of the most important variables with compounds for all models (Table S7 in Supplementary material).

## Conclusions

Michael adducts of aroylacrylic acids and cyclic amines (*N*-Me-piperazine, imidazole, 2-Me-imidazole, and indole) showed antiproliferative potency in a wide range of concentrations ($IC_{50}$ ∼ 1 to >200 μM) toward five human tumor cell lines tested in vitro (HeLa, LS174, K562, FemX, MDA-MB-361). *N*-Addition adducts obtained with *N*-Me-piperazine, imidazole, and 2-Me-imidazole appeared significantly more potent, as compared to *C*-addition adducts obtained with indole. *N*-Addition adducts having bulky alkyl substituents on the aroyl part of molecules were most active and most selective. *N*-Me-piperazine and imidazole adducts of 2,4-di-*i*-Pr-Ph benzoylacrylic acid (compounds **3** and **6**, respectively) were ∼60 and 35 times less cytotoxic toward healthy human cells, compared with K562, the most sensitive human tumor cell line tested. It should be noted that synthetic feasibility, solubility, and potency of compounds are strongly dependent on both substitution pattern on the aroyl moiety and structure of the cyclic amine. Cell cycle analysis and fluorescent staining revealed that representative compounds increase the fraction of cells in S phase, and caused apoptosis of the cells. Further biological tests to obtain more data on the main molecular target of compounds are in progress.

## Experimental

### Chemistry

All chemicals were purchased from Fluka, Aldrich, or Merck, having >98 % purity, and were used as received. For thin-layer chromatography, silica gel (63–100, 60 Å) with fluorescent indicator (254 nm) was used. Melting points were determined in open capillary tubes on an SMP-10 Stuart apparatus and are uncorrected. ESI-MS spectra were recorded in methylene chloride/methanol (1:1), or in methanol on an Agilent Technologies 6210-1210 TOF-EC-ESI-MS instrument in positive or negative mode. Mass spectra of sodium salts were not recorded. IR spectra were recorded on a Thermo Nicolet 6700 FT-IC spectrophotometer, ATR. $^{1}H$, $^{13}C$ NMR and NOESY spectra were recorded in $CDCl_3$, $CD_3OD$, $D_2O$, or DMSO-$d_6$ on Bruker AVANCE 500/125 MHz or a Varian Gemini2000 200/50 MHz instrument. Chemical shifts are reported in parts per million (*ppm*) relative to tetramethylsilane (TMS) or to 4,4-dimethyl-4-silapentane-1-sulfonic acid (DSS), and spin multiplicities are given as follows: *s* (singlet), *d* (doublet), *t* (triplet), *q* (quartet), *qv* (quintet), *m* (multiplet), *br* (broad). HR-ESI MS and NMR spectra of the compounds **1**–**21** are shown in the Supplementary materials II and III. Mixtures of stereoisomers in an unspecified proportion are represented by wavy bonds in Scheme 1 and the tables.

### General procedures for the synthesis of compounds

#### *Synthesis of 4-aryl-4-oxo-2-butenoic acids (**P1**–**P10**)*

Maleic acid anhydride (6.125 g, 0.0625 mol) and $AlCl_3$ (16.5 g, 0.125 mol) were suspended in dichloromethane (25 mL) in a 100-mL two-necked flask equipped with a reflux condenser, addition funnel, and stirring bar (Scheme 1). The mixture was stirred for 25 minutes. The corresponding substituted benzene (ethyl-benzene, *i*-Pr-benzene, *t*-Bu-benzene, *o*-xylene, *m*-xylene, *p*-xylene, tetraline, 1,3-di-*i*-Pr-benzene, 1,3,5-tri-Et-benzene, fluorobenzene), 0.0625 mol, was slowly added dropwise in a way that the reaction mixture foams slightly and turns to brownish red color. After addition of the aromatic reactant, the mixture was stirred at room temperature for 4.5 h. The reaction mixture was quenched by slowly pouring, while stirring, into a beaker with 15 mL conc. HCl and 100 g of crushed ice. A bright yellow precipitate appeared. Then dichloromethane was removed by steam distillation, the precipitate collected on a Büchner funnel and washed with cold water. The precipitate was suspended in an aqueous $Na_2CO_3$ at room temperature, till pH 8.5 was reached. The suspension was filtered through quantitative filter paper into the acidified water (HCl, pH 1) with stirring for 1 h. The precipitate was collected on the Büchner funnel, washed with cold water and dried on air. Crude products were recrystallized from the corresponding solvent. After quenching of the reaction mixture and removal of the $CH_2Cl_2$, compounds **P8** and **P9** were extracted with di-Et-ether (2 × 100 mL); the organic layer was washed with water (2 × 50 mL), dried, and concentrated under vacuo till crystals appeared. The product was recrystallized from the corresponding solvent.

*Synthesis of 4-aryl-4-oxo-2- N-cycloalkylidenbutanoic acids (**1–4**), 4-aryl-4-oxo-2-N-arylidenbutanoic acids (**5–12**) and 4-aryl-4-oxo-2-C-arylidenbutanoic acids (**13–21**)*

4-Aryl-4-oxo-2-butenoic acids (**P1**–**P10**) were dissolved in 20-35 mL mixture of dichloromethane/toluene (3:1) in a 50-mL flask equipped with a reflux condenser and stirring bar. Then, 1.2 molar equivalent of secondary amine (*N*-methylpiperazine, imidazole, 2-methyl-1*H*-imidazole) was added. The mixture was stirred at room temperature until it appeared turbid. Then stirring was continued at room temperature for additional 2.5–3 h. The reaction was monitored by TLC. Upon completion of the reaction, the mixture was evaporated to about 1/8 of the initial volume, and the crude product rinsed with diethyl ether on the funnel, then dried in air.

4-Aryl-4-oxo-2-*C*-arylidenbutanoic acids (**13**–**21**) were obtained in reaction of 4-aryl-4-oxo-2-butenoic acids with 1.2 molar equivalent of 1*H*-indole, in 20–35 mL dichloromethane/toluene (3:1) mixture in a 50-mL flask equipped with a reflux condenser and stirring bar. The mixture was stirred at room temperature until turbidity appeared. Then stirring was continued at room temperature for additional 24 h. Compound **20** was obtained after three days of mixing of reagents. Reactions were monitored by TLC. Upon reaction completion, the mixture was evaporated to about 1/8 of the initial volume. The crude product was rinsed with diethyl ether on the funnel, then dried in air. Isolated yields of **1**–**21** are reported in the characterization section below.

*Synthesis of 4-aryl-4-oxo-2- N-cycloalkylidenbutanoic acid sodium salt (**1a**) and 4-aryl-4-oxo-2-N-arylidenbutanoic acids sodium salts (**5a** and **7a–12a**)*

4-Aryl-4-oxo-2-*N*-cycloalkylidenbutanoic acid (**1**) or 4-aryl-4-oxo-2-*N*–arylidenbutanoic acids (**5, 7**–**12**) were dissolved, or suspended, in 4 ml MeOH, in a 50-mL flask equipped with a stirring bar. Then an equimolar amount of aqueous 0.1 M NaOH was added dropwise. The mixture was stirred at room temperature for 24 h and then evaporated to dryness. Obtained 4-aryl-4-oxo-2-*N*-cycloalkylidenbutanoic acid sodium salt (**1a**) and 4-aryl-4-oxo-2-*N*-arilydenbutanoic acids sodium salts (**5a, 7a**–**12a**) were characterized by $^{1}$H and $^{13}$C NMR spectroscopy and infrared spectroscopy.

Characterization of compounds

*(E)-4-(4-Fluorophenyl)-4-oxo-2-butenoic acid (**P1**)*

$C_{10}H_7FO_3$, starting from maleic acid anhydride (6.125 g, 0.0625 mol) and a corresponding amount of fluorobenzene (5.86 mL, 0.0625 mol), 10.92 g **P1** was obtained, 90 % yield, yellow solid, m.p. 142 °C (PhH). $^{1}$H NMR (200 MHz, $CDCl_3$) $\delta$ = 6.38 (*d*, 1H, *J* = 15.17 Hz, Ar–C(O)–C<u>H</u>=CH–COOH); 7.19 (*t*, 2H, *J* = 8.98 Hz, 3,5-C<u>H</u>–Ar); 7.97 (*d*, 1H, *J* =15.72, Ar–C(O)–CH=C<u>H</u>–COOH); 8.05 (*m*, 2H, 2,6-C<u>H</u>–Ar); 11.24 (*s*, *b*, 1H, –COO<u>H</u>). $^{13}$C NMR (50 MHz, $CDCl_3$) $\delta$ = 116.05; 116.49; 131.60; 131.80; 132.77; 132.82; 138.08; 163.81; 168.93; 170.73; 187.59. IR ($\nu$, $cm^{-1}$): 1667 (Ar–<u>C(O)</u>–), 1711 (–<u>C(O)</u>–OH). HR MS (ESI): 195.0452 (M+1), Calc. 195.0457.

*(E)-4-(4-Ethylphenyl)-4-oxo-2-butenoic acid (**P2**)*

$C_{12}H_{12}O_3$, starting from maleic acid anhydride (6.125 g, 0.0625 mol) and a corresponding amount of ethylbenzene (7.66 mL, 0.0625 mol), 10.98 g **P2** was obtained, 86 % yield, yellow solid, m.p. 106–107 °C (PhH). $^{1}$H NMR (200 MHz, $CDCl_3$) $\delta$ = 1.26 (*t*, 3H, *J* = 7.64 Hz, 4-$CH_2-C\underline{H}_3$); 2.71 (*q*, 2H, $J_{1,2}$ = 7.64 Hz, $J_{1,3}$ = 15.07 Hz, 4-C<u>H</u>$_2$–$CH_3$); 6.89 (*d*, 1H, *J* = 15.48 Hz, Ar–C(O)–C<u>H</u>=CH–COOH); 7.32 (*d*, 2H, *J*= 7.32 Hz, 3,5-C<u>H</u>–Ar); 7.93 (*d*, 2H, *J* = 8.25 Hz, 2,6-C<u>H</u>–Ar); 8.01 (*d*, 1H, *J* = 15.48 Hz, Ar–C(O)–CH=C<u>H</u>–COOH); 12.33 (*s*, *b*, 1H, –COO<u>H</u>). $^{13}$C NMR (50 MHz, $CDCl_3$) $\delta$ = 14.81; 28.81; 128.31; 129.09; 131.06; 133.88; 138.19; 151.25; 170.62; 188.66. IR ($\nu$, $cm^{-1}$): 1669 (Ar–<u>C(O)</u>–), 1701 (–<u>C(O)</u>–OH). HR MS (ESI): 205.0858 (M+1), Calc. 205.0865.

*(E)-4-(4-Isopropyphenyl)-4-oxo-2-butenoic acid (**P3**)*

$C_{13}H_{14}O_3$, starting from maleic acid anhydride (6.125 g, 0.0625 mol) and a corresponding amount of isopropylbenzene (8.71 mL, 0.0625 mol), 9.55 g **P3** was obtained, 70 % yield, yellow solid, m.p. 102–103 °C (PhH). $^{1}$H NMR (200 MHz, $CDCl_3$) $\delta$ = 1.25 (*d*, 6H, *J* = 7.30 Hz, 4-CH–(C<u>H</u>$_3$)$_2$); 2.97 (*h*, 1H, $J_{1,2}$ = 6.74 Hz, $J_{1,3}$ = 13.48 Hz, 4-C<u>H</u>–$(CH_3)_2$); 6.88 (*d*, 1H, *J* = 15.73 Hz Ar–C(O)–C<u>H</u>=CH–COOH); 7.35 (*d*, 2H, *J* = 8.42 Hz, 3,5-C<u>H</u>–Ar); 7.94 (*d*, 2H, *J* = 8.43 Hz, 2,6-C<u>H</u>–Ar); 8.00 (*d*, 1H, *J* = 15.70 Hz, Ar–C(O)–CH=C<u>H</u>–COOH); 11.95 (*s*, *b*, 1H, –COO<u>H</u>). $^{13}$C NMR (50 MHz, $CDCl_3$) $\delta$ = 23.45; 34.23; 127.01; 129.22; 131.17; 134.13; 138.43; 155.87; 170.84; 188.79. IR ($\nu$, $cm^{-1}$): 1662 (Ar–<u>C(O)</u>–), 1698 (–<u>C(O)</u>–OH). HR MS (ESI): 219.1012 (M+1), Calc. 219.1021.

*(E)-4-(4-Tertbutylphenyl)-4-oxo-2-butenoic acid (**P4**)*

$C_{14}H_{16}O_3$, starting from maleic acid anhydride (6.125 g, 0.0625 mol) and a corresponding amount of *tert*-butylbenzene (9.67 mL, 0.0625 mol), 10.45 g **P4** was obtained, 72 % yield, yellow solid, m.p. 125–127 °C (PhH).$^{1}$H NMR (200 MHz, $CDCl_3$) $\delta$ = 1.24 (*s*, 9H, 4-C(C<u>H</u>$_3$)$_3$); 6.99 (*d*, 1H, *J* = 15.17 Hz, Ar–C(O)–C<u>H</u>=CH–COOH); 7.52 (*d*, 2H, *J* = 8.43 Hz, 3,5-C<u>H</u>–Ar); 7.95 (*d*, 2H, *J* = 7.86 Hz, 2,6-

CH–Ar); 8.03 (*d*, 1H, *J* = 15.16 Hz, Ar–C(O)–CH=CH–COOH); 12.03 (*s*, *b*, 1H, –COOH). $^{13}$C NMR (50 MHz, $CDCl_3$) $\delta$ = 30.90; 35.18; 125.90; 128.94; 131.15; 133.71; 138.48; 158.13; 170.93; 188.79. IR($\nu$, $cm^{-1}$): 1663 (Ar–C(O)–), 1698 (–C(O)–OH). HR MS (ESI): 233.1180 (M+1), Calc. 233.1178.

*(E)-4-(2,4-Dimethylphenyl)-4-oxo-2-butenoic acid (**P5**)*

$C_{12}H_{12}O_3$, starting from maleic acid anhydride (6.125 g, 0.0625 mol) and a corresponding amount of *m*-xylene (7.71 mL, 0.0625 mol), 9.06 g **P5** was obtained, 71 % yield, yellow solid, m.p. 110–111 °C (EtOH). $^1$H NMR (200 MHz, $CDCl_3$) $\delta$ = 2.35 (*s*, 3H, 4-CH$_3$–Ar); 2.48 (*s*, 3H, 2-CH$_3$–Ar); 6.69 (*d*, 1H, *J* = 15.72 Hz, Ar–C(O)–CH=CH–COOH); 7.09 (*b*, 2H, 3,5-CH–Ar); 7.54 (*d*, 2H, *J* = 8.43 Hz, 6-CH–Ar); 7.74 (*d*, 1H, *J* = 15.73 Hz, Ar–C(O)–CH=CH–COOH); 11.86 (*s*, *b*, 1H, –COOH). $^{13}$C NMR (50 MHz, $CDCl_3$) $\delta$ = 21.09; 21.36; 126.38; 130.04; 130.91; 132.93; 133.48; 139.45; 141.60; 143.13; 170.95; 192.45. IR ($\nu$, $cm^{-1}$): 1670 (Ar–C(O)–), 1716 (–C(O)–OH). HR MS (ESI): 205.0856 (M+1), Calc. 205.0865.

*(E)-4-(2,5-Dimethylphenyl)-4-oxo-2-butenoic acid (**P6**)*

$C_{12}H_{12}O_3$, starting from maleic acid anhydride (6.125 g, 0.0625 mol) and a corresponding amount of *p*-xylene (7.71 mL, 0.0625 mol), 12.13 g **P6** was obtained, 95 % yield, yellow solid, m.p. 76–78 °C (EtOH). $^1$H NMR (200 MHz, $CDCl_3$) $\delta$ = 2.37 (*s*, 3H, 5-CH$_3$–Ar); 2.45 (*s*, 3H, 2-CH$_3$–Ar); 6.70 (*d*, 1H, *J* = 15.72 Hz, Ar–C(O)–CH=CH–COOH); 7.17 (*d*, 1H, *J* = 7.86 Hz, 3-CH–Ar); 7.24 (*d*, 1H, *J* = 7.87 Hz, 4-CH–Ar); 7.40 (*s*, 1H, 6-CH–Ar); 7.71 (*d*, 1H, *J* = 15.72 Hz, Ar–C(O)–CH=CH–COOH); 11.99 (*s*, *b*, 1H, –COOH). $^{13}$C NMR (50 MHz, $CDCl_3$) $\delta$ = 20.36; 20.76; 129.85; 131.27; 131.89; 132.95; 135.39; 135.64; 136.34; 147.73; 171.04; 193.51. IR ($\nu$, $cm^{-1}$): 1674 (Ar–C(O)–), 1712 (–C(O)–OH). HR MS (ESI): 203.0708 (M−1), Calc. 203.0708.

*(E)-4-(3,4-Dimethylphenyl)-4-oxo-2-butenoic acid (**P7**)*

$C_{12}H_{12}O_3$, starting from maleic acid anhydride (6.125 g, 0.0625 mol) and a corresponding amount of *o*-xylene (7.71 mL, 0.0625 mol), 9.19 g **P7** was obtained, 72 % yield, yellow solid, m.p. 121–121.5 °C (EtOH). $^1$H NMR (200 MHz, $CDCl_3$) $\delta$ = 2.33 (*s*, 6H, 3,5-CH$_3$–Ar); 6.86 (*d*, 1H, *J* = 15.17 Hz, Ar–C(O)–CH=CH–COOH); 7.25 (*d*, 1H, *J* = 7.87 Hz, 6-CH–Ar); 7.71–7.77 (*m*, 2H, 2,5-CH–Ar); 7.98 (*d*, 1H, *J* = 15.72 Hz, Ar–C(O)–CH=CH–COOH); 11.50 (*s*, *br*, 1H, –COOH). $^{13}$C NMR (50 MHz, $CDCl_3$) $\delta$ = 19.72; 20.12; 126.67; 129.98; 130.16; 130.93; 134.28; 137.50; 138.70; 144.09; 170.98; 188.92. IR ($\nu$, $cm^{-1}$): 1669 (Ar–C(O)–), 1716 (–C(O)–OH). HR MS (ESI): 205.0848 (M+1), Calc. 205.0865.

*(E)-4-(2,4-Diisopropylphenyl)-4-oxo-2-butenoic acid (**P8**)*

$C_{16}H_{20}O_3$, starting from maleic acid anhydride (6.125 g, 0.0625 mol) and a corresponding amount of 1,3-diisopropylbenzene (11.90 mL, 0.0625 mol), 11.39 g **P8** was obtained, 70 % yield, yellow solid, m.p. 113–113.5 °C (cyclohexane). $^1$H NMR (500 MHz, $CDCl_3$) $\delta$ = 1.25 (*d*, 6H, *J* = 6.97 Hz, 4-CH–(CH$_3$)$_2$); 1.275 (*d*, 6H, *J* = 6.97 Hz, 2-CH–(CH$_3$)$_2$); 2.95 (*h*, 1H, $J_{1,2}$ = 6.97 Hz, $J_{1,3}$ = 13.94 Hz, 4-CH–(CH$_3$)$_2$); 3.38 (*h*, 1H, $J_{1,2}$ = 6.60 Hz, $J_{1,3}$ = 13.57 Hz, 2-CH–(CH$_3$)$_2$); 6.63 (*d*, 1H, *J* = 15.78 Hz, Ar–C(O)–CH=CH–COOH); 7.13 (*dd*, 1H, $J_{1,2}$ = 1.47 Hz, $J_{1,3}$ = 8.07 Hz, 5-CH–Ar); 7.29 (*s*, 1H, 3-CH–Ar); 7.39 (*d*, 1H, *J* = 8.07 Hz, 6-CH–Ar); 7.61 (*d*, 1H, *J* = 15.78 Hz, Ar–C(O)–CH=CH–COOH); 11.00 (*s*, *b*, 1H, –COOH). $^{13}$C NMR (125 MHz, $CDCl_3$) $\delta$ = 23.72; 24.10; 29.62; 34.40; 123.44; 124.94; 128.92; 131.13; 134.23; 142.63; 149.16; 153.26; 170.58; 194.47. IR ($\nu$, $cm^{-1}$): 1673 (–C(O)–OH), 1702 (Ar–C(O)–). HR MS (ESI): 259.1335 (M−1), Calc. 259.1334.

*(E)-4-(2,4,6-Triethylphenyl)-4-oxo-2-butenoic acid (**P9**)*

$C_{16}H_{20}O_3$, starting from maleic acid anhydride (6.125 g, 0.0625 mol) and a corresponding amount of 1,3,5-triethylbenzene (11.76 mL, 0.0625 mol), 10.57 g **P9** was obtained, 65 % yield, yellow solid, m.p. 96–97 °C (petroleum-ether). $^1$H NMR (500 MHz, $CDCl_3$) $\delta$ = 1.13 (*t*, 6H, *J* = 7.71 Hz, 2,6-CH$_2$–CH$_3$); 1.24 (*t*, 3H, *J* = 7.21 Hz, 4-CH$_2$–CH$_3$); 2.44 (*q*, 4H, $J_{1,2}$ = 7.70 Hz, $J_{1,3}$ = 15.04 Hz, 2,6-CH$_2$–CH$_3$); 2.63 (*q*, 2H, $J_{1,2}$ = 7.70 Hz, $J_{1,3}$ = 15.40 Hz, 4-CH$_2$–CH$_3$); 6.37 (*d*, 1H, *J* = 16.14 Hz, Ar–C(O)–CH=CH–COOH); 6.93 (*s*, 2H, 3,5-CH–Ar); 7.31 (*d*, 1H, *J* = 16.14 Hz, Ar–C(O)–CH=CH–COOH); 11.40 (*s*, 1H, –COOH). $^{13}$C NMR (125 MHz, $CDCl_3$) $\delta$ = 15.35; 15.72; 26.39; 28.76; 125.87; 132.35; 134.97; 140.57; 143.49; 146.04; 170.62; 200.13. IR ($\nu$, $cm^{-1}$): 1668 (Ar–C(O)–), 1703 (–C(O)–OH). HR MS (ESI): 259.1367 (M−1), Calc. 259.1334.

*(E)-4-(5,6,7,8-Tetrahydronaphtalene-2-yl)-4-oxo-2-butenoic acid (**P10**)*

$C_{14}H_{14}O_3$, starting from maleic acid anhydride (6.125 g, 0.0625 mol) and a corresponding amount of tetraline (8.52 mL, 0.0625 mol), 10.07 g **P10** was obtained, 70 % yield, yellow solid, m.p. 147–149 °C (PhH). $^1$H NMR (500 MHz, $CDCl_3$) $\delta$ = 1.82 (*m*, 4H, 3,4-(CH$_2$–CH$_2$)–); 2.82 (*m*, 4H, 3,4-(CH$_2$–CH$_2$)–); 6.86 (*d*, 1H, *J* =15.44 Hz, Ar–C(O)–CH=CH–COOH); 7.18 (*d*, 1H, *J* = 8.61 Hz, 5-CH–Ar); 7.70–7.72 (*m*, 2H, 2,6-CH–Ar); 7.98 (*d*, 1H, *J* = 15.45 Hz, Ar–C(O)–CH=CH–COOH); 11.26 (*s*, *b*, 1H, –COOH).

$^{13}$C NMR (125 MHz, $CDCl_3$) $\delta$ = 22.78; 22.93; 29.42; 29.85; 125.82; 129.55; 129.66; 130.73; 133.67; 137.79; 138.51; 144.45; 170.60; 188.63. IR ($\nu$, $cm^{-1}$): 1671 (Ar–C(O)–), 1700 (–C(O)–OH); HR MS (ESI): 231.1014 (M+1), Calc. 231.1021.

*(2R,S)-4-(4-Tertbutylphenyl)-2-(4-methylpiperazine-1-yl)-4-oxobutanoic acid (**1**)*

$C_{19}H_{28}N_2O_3$, starting from (*E*)-4-(4-*tert*-butylphenyl)-4-oxo-2-butenoic acid (0.00215 mol, 0.5 g) and an *N*-methylpiperazine (0.00258 mol, 0.286 mL), 0.688 g **1** was obtained, 96.22 % yield, light yellow solid, m.p. 160 °C decomposition, ($CH_2Cl_2$/$PhCH_3$). $^1$H NMR (500 MHz, $CD_3OD$) $\delta$ = 1.34 (*s*, 9H, Ar-4-C(C$\underline{H}_3$)$_3$); 2.72 (*s*, *b*, 3H, *N*-C$\underline{H}_3$); 2.89–2.91 (*d,br*, 8H, piperazine-C$\underline{H}_2$–); 3.07–3.09 (*d*, *br*, 1H, *J* = 5.65 Hz); 3.17 (triplet like signal, 1H, *J* = 5.22 Hz); 3.79 (*d*, 1H, *J* = 6.81 Hz); 7.53 (*d*, 2H, *J* = 8.55 Hz, 2,6-C$\underline{H}$–Ar); 7.94 (*d*, 2H, *J* = 8.55 Hz, 3,5-C$\underline{H}$–Ar). $^{13}$C NMR (125 MHz, $CD_3OD$) $\delta$ = 31.62; 36.10; 43.41; 44.75; 53.21; 55.22; 67.17; 126.79; 129.35; 136.01; 158.28; 176.85; 200.33. HR MS (ESI): 333.2173 (M+1), Calc. 333.2178.

*Sodium-(2R,S)-4-(4-tertbutylphenyl)-2-(4-methylpiperazine-1-yl)-4-oxobutanoate (**1a**)*

$C_{19}H_{27}N_2NaO_3$, starting from (2*R*,*S*)-4-(4-*tert*-butylphenyl)-2-(4-methylpiperazine-1-yl)-4-oxobutanoic acid (**1**) (0.00045 mol, 0.15 g) and an equimolar amount of NaOH (0.1 M), 0.077 g **1a** was obtained, 48 % yield, orange solid. $^1$H NMR (200 MHz, $D_2O$)$\delta$ = 1.25 (*s*, 9H, Ar-4-C(C$\underline{H}_3$)$_3$); 2.24 (*s*, 3H, *N*-C$\underline{H}_3$); 2.92 (*dd*, 1H, $J_{1,2}$ = 5.05 Hz, $J_{1,3}$= 10.11 Hz); 3.28 (*d, br*, 1H, *J* = 5.62 Hz); 3.47 (*s*, 8H, piperazine-C$\underline{H}_2$–); 3.72 (*dd*, 1H, $J_{1,2}$ = 3.93 Hz, $J_{1,3}$ = 7.30 Hz); 7.45 (*d*, 2H, *J* = 8.42 Hz, 2,6-C$\underline{H}$–Ar); 7.96 (*d*, 2H, *J* = 8.42 Hz, 3,5-C$\underline{H}$–Ar). $^{13}$C NMR (50 MHz, $D_2O$) $\delta$ = 32.88; 36.74; 46.01; 46.66; 51.05; 56.24; 68.77; 127.63; 130.58; 136.46; 158.78; 179.06; 203.43. IR ($\nu$, $cm^{-1}$): 1607.6 (Ar–C(O)–), 1680 (–C(O)–OH).

*(2R,S)-4-(2,5-Dimethylphenyl)-2-(4-methylpiperazine-1-yl)-4-oxobutanoic acid (**2**)*

$C_{17}H_{24}N_2O_3$, starting from (*E*)-4-(2,5-dimethylphenyl)-4-oxo-2-butenoic acid (0.00245 mol, 0.5 g) and an *N*-methylpiperazine (0.00294 mol, 0.33 mL), 0.392 g **2** was obtained, 52.55 % yield, light yellow solid, m.p. 157 °C decomposition, ($CH_2Cl_2$/$PhCH_3$).$^1$H NMR (200 MHz, $CDCl_3$) $\delta$ = 2.33(*s*, 3H, 5-C$\underline{H}_3$–Ar); 2.42 (*s*, 3H, 2-C$\underline{H}_3$–Ar); 2.53 (*s*, 3H, *N*-C$\underline{H}_3$); 2.67–2.85 (*d, br,* 8H, piperazine-C$\underline{H}_2$–); 3.10 (*dd*, 1H, $J_{1,2}$ = 7.30 Hz, $J_{1,3}$= 16.29 Hz); 3.38 (*dd*, 1H, $J_{1,2}$ = 8.99 Hz, $J_{1,3}$ = 15.72 Hz); 3.72 (*dd*, 1H, $J_{1,2}$ = 6.74 Hz, $J_{1,3}$ = 15.16 Hz); 7.11 (*t*, *br*, 2H, 3,4-C$\underline{H}$–Ar); 7.43 (*s*, 1H, 6-C$\underline{H}$–Ar). $^{13}$C NMR (50 MHz, $CDCl_3$) $\delta$ = 20.36; 20.78; 42.10; 42.90; 50.23; 53.68; 65.27; 128.63; 131.46; 134.30; 134.90; 138.26; 174.31; 203.39. IR ($\nu$, $cm^{-1}$): 1629.5 (Ar–C(O)–), 1692.8 (–C(O)–OH). HR MS (ESI): 305.1714 (M+1), Calc. 305.1865; 303.1725 (M−1), Calc. 303.1709

*(2R,S)-4-(2,4-Diisopropylphenyl)-2-(4-methylpiperazine-1-yl)-4-oxobutanoic acid (**3**)*

$C_{21}H_{32}N_2O_3$, starting from (*E*)-4-(2,4-diisopropylphenyl)-4-oxo-2-butenoic acid (0.002 mol, 0.5 g) and an *N*-methylpiperazine (0.0024 mol, 0.27 mL), 0.542 g **3** was obtained, 75.17 % yield, light yellow solid, m.p. 136 °C ($CH_2Cl_2$/$PhCH_3$). $^1$H NMR (200 MHz, $CDCl_3$) $\delta$= 1.22 (singlet like signal, 6H, 2-CH–(C$\underline{H}_3$)$_2$); 1.25 (singlet like signal, 6H, 4-CH–(C$\underline{H}_3$)$_2$); 2.54 (*s*, 3H, *N*-C$\underline{H}_3$); 2.84–3.07 (*m*, 9H, piperazine-C$\underline{H}_2$ and 2-C$\underline{H}$(CH$_3$)$_2$); 3.34–3.51 (*m*, 3H, 4-C$\underline{H}$–(CH$_3$)$_2$); 3.75 (*t*, *b*, 1H, *J*= 0.04 Hz); 7.06 (*d*, 1H, *J*= 7.86 Hz, 3-C$\underline{H}$–Ar); 7.22 (*s*, 1H, 5-C$\underline{H}$–Ar); 7.47 (*d*, 1H, *J*= 7.86 Hz, 6-C$\underline{H}$–Ar). $^{13}$C NMR (50 MHz, $CDCl_3$) $\delta$ = 23.71; 24.38; 29.06; 34.16; 42.95; 43.17; 53.93; 65,24; 123.12; 124.48; 127.76; 136.44; 147.91; 151.72; 174.39; 204.14. IR ($\nu$, $cm^{-1}$): 1606,6 (Ar–C(O)–), 1681,5 (–C(O)–OH). HR MS (ESI): 361.2344 (M+1), Calc. 361.2491; 359.2353 (M−1), Calc. 359.2335.

*(2R,S)-4-(5,6,7,8-Tetrahydronaphtalene-2-yl)-2-(4-methylpiperazine-1-yl)-4-oxobutanoic acid (**4**)*

$C_{19}H_{26}N_2O_3$, starting from (*E*)-4-(5,6,7,8-tetrahydronaphtalene-2-yl)-4-oxo-2-butenoic acid (0.00217 mol, 0.5 g) and an *N*-methylpiperazine (0.0026 mol, 0.29 mL), 0.520 g **4** was obtained, 72.52 % yield, light yellow solid, m.p. 176 °C decomposition, ($CH_2Cl_2$/$PhCH_3$).$^1$H NMR (200 MHz, $CDCl_3$) $\delta$ = 1.80 (singlet like signal, 4H, 3,4-(CH$_2$–C$\underline{H}_2$)–); 2.54 (*s*, 3H, *N*-C$\underline{H}_3$); 2.79–2.88 (*m*, 12H, 3,4-(C$\underline{H}_2$–CH$_2$)– and piperazine-C$\underline{H}_2$); 3.09 (*dd*, 1H, $J_{1,2}$= 8.99 Hz, $J_{1,3}$= 16.29 Hz); 3.52 (*dd*, 1H, $J_{1,2}$= 8.99 Hz, $J_{1,3}$= 16.29 Hz); 3.86 (*t*, 1H, *J*= 7.30 Hz); 7.11 (doublet like signal, 1H, *J*= 8.42, 5-C$\underline{H}$–Ar); 7.86 (singlet like signal, 2H, 2,6-C$\underline{H}$–Ar).$^{13}$C NMR (50 MHz, $CDCl_3$) $\delta$ = 22.81; 22.94; 29.33; 29.57; 39.26; 43.04; 64.80; 125.19; 129.05; 129.23; 134.68; 137.26; 142.85; 174.62; 198.44. IR ($\nu$, $cm^{-1}$): 1631.3 (Ar–C(O)–), 1679.1 (–C(O)–OH). HR MS (ESI): 331.1874 (M+1), Calc. 331.2022; 329.1883 (M−1), Calc. 329.1865

*(2R,S)-4-(2,5-Dimethylphenyl)-2-(1H-imidazole-1-yl)-4-oxobutanoic acid (**5**)*

$C_{15}H_{16}N_2O_3$, starting from (*E*)-4-(2,5-dimethylphenyl)-4-oxo-2-butenoic acid (0.00245 mol, 0.5 g) and imidazole

(0.00284 mol, 0.193 g), 0.523 g **5** was obtained, 78.39 % yield, light yellow solid, m.p. 123 °C ($CH_2Cl_2$/$PhCH_3$).$^1$H NMR (500 MHz, $CD_3OD$) $\delta$ = 1.24 (*s*, 3H, 5-C<u>H</u>$_3$–Ar); 1.26 (*s*, 3H, 2-C<u>H</u>$_3$–Ar); 2.95 (*qv*, 1H, $J_{1,2}$= 6.89 Hz, $J_{1,3}$= 13.80 Hz); 3.96 (*dd*, 1H, $J_{1,2}$= 12.05 Hz, $J_{1,3}$= 21.57 Hz); 5.48 (*t*,*br*, 1H, $J_{1,2}$= 9.52 Hz); 7.35 (*s*, 1H, 4-C<u>H</u>–imidazole); 7.36 (*s*, 1H, 3-C<u>H</u>–Ar); 7.38 (*s*, 1H, 5-C<u>H</u>–imidazole); 7.62 (*s*, 1H, 2-C<u>H</u>–imidazole); 7.91 (*s*, 1H, 6-C<u>H</u>–Ar); 7.92 (*s*, 1H, 4-C<u>H</u>–Ar); 8.83 (*s*, 1H, –COO<u>H</u>). $^{13}$C NMR (125 MHz, $CD_3OD$) $\delta$ = 24.15; 35.64; 42.69; 61.33; 121.56; 122.94; 128.03; 129.67; 135.58; 137.61; 156.78; 173.51; 197.97. HR MS (ESI): 273.1143 (M+1), Calc. 273.1239.

*Sodium-(2R,S)-4-(2,5-dimethylphenyl)-2-(1H-imidazole-1-yl)-4-oxobutanoate (**5a**)*

$C_{15}H_{15}N_2NaO_3$, starting from (2*R*,*S*)-4-(2,5-dimethylphenyl)-2-(1*H*-imidazole-1-yl)-4-oxobutanoic acid (**5**) (0.00073 mol, 0.2 g) and an equimolar amount of NaOH (0.1 M), 0.145 g **5a** was obtained, 67.38 % yield, light yellow solid.$^1$H NMR (200 MHz, $D_2O$) $\delta$ = 1.10 (*s*, 3H, 5-C<u>H</u>$_3$–Ar); 1.13 (*s*, 3H, 2-C<u>H</u>$_3$–Ar); 2.78–2.97 (*m*, 1H); 3.78 (*dd*, 1H, $J_{1,2}$= 7.86 Hz, $J_{1,3}$= 16.85 Hz); 5.35 (*t*, *br*, 1H, *J*= 5.62 Hz); 7.03 (*s*,1H, 4-C<u>H</u>–imidazole); 7.24 (singlet like signal, 3H, *J* = 8.42 Hz, 3,4-C<u>H</u>–Ar and 5-C<u>H</u>–imidazole); 7.75 (*d*, 1H, *J* = 8.42 Hz, 6-C<u>H</u>–Ar); 7.85–7.95 (*d, br*, 1H, 2-C<u>H</u>–imidazole). $^{13}$C NMR (50 MHz, $D_2O$) $\delta$ = 25.54; 36.41; 60.97; 122.24; 129.58; 131.24; 136.22; 158.78; 178.26; 202.28. IR ($\nu$, $cm^{-1}$): 1603.2 (Ar-<u>C(O)</u>-), 1678.7 (-<u>C(O)</u>-OH).

*(2R,S)-4-(2,4-Diisopropylphenyl)-2-1H(-imidazole-1-yl)-4-oxobutanoic acid (**6**)*

$C_{19}H_{24}N_2O_3$, starting from (*E*)-4-(2,4-diisopropylphenyl)-4-oxo-2-butenoic acid (0.002 mol, 0.5 g) and imidazole (0.0024 mol, 0.163 g), 0.443 g **6** was obtained, 67.43 % yield, light yellow solid, m.p. 142 °C ($CH_2Cl_2$/$PhCH_3$). $^1$H NMR (200 MHz, $CDCl_3$) $\delta$ = 1.08 (*d*, 3H, *J*= 7.30 Hz, 2-CH-(C<u>H</u>$_3$)$_2$); 1.16 (*d*, 3H, *J*= 6.74 Hz, 2-CH-(C<u>H</u>$_3$)$_2$); 1.22 (*d*, 6H, *J*= 7.30 Hz, 4-CH-(C<u>H</u>$_3$)$_2$); 2.89 (*qv*, 1H, $J_{1,2}$= 6.74 Hz, $J_{1,3}$= 13.48 Hz, 4-C<u>H</u>-(CH$_3$)$_2$); 3.32 (*qv*, 1H, $J_{1,2}$= 7.30 Hz, $J_{1,3}$= 14.04 Hz, 2-C<u>H</u>-(CH$_3$)$_2$); 3.63 (*dd*, 1H, $J_{1,2}$= 8.42 Hz, $J_{1,3}$= 17.97 Hz); 3.98 (*dd*, 1H, $J_{1,2}$= 14.60 Hz, $J_{1,3}$= 17.97 Hz); 5.47 (*dd*, 1H, $J_{1,2}$= 6.18 Hz, $J_{1,3}$= 10.11 Hz); 7.05 (*d*, 1H, *J*= 7.86 Hz, 3-C<u>H</u>–Ar); 7.11 (*s*, 1H, 4-C<u>H</u>–imidazole); 7.21–7.27 (*m*, 2H, 5-C<u>H</u>–imidazole and 5-C<u>H</u>–Ar); 7.45 (*d*, 1H, *J*= 7.87 Hz, 6-C<u>H</u>–Ar); 8.45 (*s*, *b*, 1H, 2-C<u>H</u>–imidazole); 10.47 (*s*, *b*, 1H, -C(O)-O<u>H</u>). $^{13}$C NMR (50 MHz, $CDCl_3$) $\delta$ = 23.63; 23.93; 24.05; 28.93; 34.25; 45.81; 59.39; 119.02; 120.77; 121.70; 123.43; 124.90; 128.29; 134.59; 136.17; 148.88; 153.01; 172.51; 200.62. IR ($\nu$, $cm^{-1}$): 1603.9 (Ar-<u>C(O)</u>-), 1680.0 (–<u>C(O)</u>–OH). HR MS (ESI): 329.1869 (M+1), Calc. 329.1865.

*(2R,S)-4-(5,6,7,8-Tetrahydronaphtalene-2-yl)-2-(1H-imidazole-1-yl)-4-oxobutanoic acid (**7**)*

$C_{17}H_{18}N_2O_3$, starting from (*E*)-4-(5,6,7,8-tetrahydronaphtalene-2-yl)-4-oxo-2-butenoic acid (0.00217 mol, 0.5 g) and imidazole (0.00253 mol, 0.172 g), 0.506 g **7** was obtained, 78.21 % yield, light brown solid, m.p. 157 °C ($CH_2Cl_2$/$PhCH_3$). Insoluble in DMSO or $CHCl_3$, converted to sodium salt.

*Sodium-(2R,S)-4-(5,6,7,8-tetrahydronaphtalene-2-yl)-2-(1H-imidazole-1-yl)-4-oxobutanoate (**7a**)*

$C_{17}H_{17}N_2NaO_3$, starting from (2*R*,*S*)-4-(5,6,7,8-tetrahydronaphtalene-2-yl)-2-(1*H*-imidazole-1-yl)-4-oxobutanoic acid (**7**) (0.00067 mol, 0.2 g) and an equimolar amount of NaOH (0.1 M), 0.132 g of **7a** was obtained, 61 % yield, brown solid. $^1$H NMR (200 MHz, $D_2O$) $\delta$ = 1.49 (*s*, 4H, 3,4-(CH$_2$–C<u>H</u>$_2$)–); 2.45 (*s*, 4H, 3,4-(C<u>H</u>$_2$–CH$_2$)–); 3.00 (*t*, *br*, 1H, *J*= 7.86 Hz); 3.85 (*d*, *b*, 1H, *J*= 9.55 Hz); 5.50 (*t*, *br*, 1H, *J*= 5.05 Hz); 6.82 (*d*, 1H, *J*= 7.86 Hz, 4-C<u>H</u>–imidazole); 7.14 (*s*, 1H, 5-C<u>H</u>–Ar); 7.38 (doublet like signal, 2H, *J*= 12.92 Hz, 2-C<u>H</u>–Ar and 5-C<u>H</u>–imidazole); 7.51 (*d*, 1H, *J*= 7.30 Hz, 6-C<u>H</u>–Ar); 8.11 (*s*, 1H, 2-C<u>H</u>–imidazole).$^{13}$C NMR (50 MHz, $D_2O$) $\delta$ = 24.98; 25.11; 31.24; 31.70; 44.81; 60.77; 122.10; 123.75; 127.87; 131.31; 131.65; 135.79; 139.52; 140.30; 145.86; 177.99; 200.66. IR ($\nu$, $cm^{-1}$): 1607.1 (Ar–<u>C(O)</u>–), 1678.2 (–<u>C(O)</u>–OH).

*(2R,S)-4-(2,4,6-Triethylphenyl)-2-(1H-imidazole-1-yl)-4-oxobutanoic acid (**8**)*

$C_{19}H_{24}N_2O_3$, starting from (*E*)-4-(2,4,6-triethylphenyl)-4-oxo-2-butenoic acid (0.00192 mol, 0.5 g) and imidazole (0.0023 mol, 0.157 g), 0.431 g of **8** was obtained, 68.41 % yield, light yellow solid, m.p. 143 °C ($CH_2Cl_2$/$PhCH_3$). $^1$H NMR (200 MHz, $CD_3OD$) $\delta$ = 1.02–1.23 (*m*, 9H, 2,4,6-CH$_2$–C<u>H</u>$_3$); 2.20–2.64 (*m*, 6H, 2,4,6-C<u>H</u>$_2$–CH$_3$); 3.68 (*d*, *br*, 1H, *J*= 7.86 Hz); 3.71 (*d*, *br*, 1H, *J*= 3.93 Hz); 4.78 (*s*, *br*, 1H); 5.49–5.55 (*m*, 1H, 4-C<u>H</u>–imidazole); 6.91 (*s*, *br*, 2H, 3,5-C<u>H</u>–Ar); 7.38–7.42 (*m*, 1H, 5-C<u>H</u>–imidazole); 7.66 (*t*, 1H, *J*= 1.68 Hz, 2-CH–imidazole); 8.86 (*s*, 1H, -C(O)-O<u>H</u>). $^{13}$C NMR (50 MHz, $CD_3OD$) $\delta$ = 16.44; 26.93; 27.37; 29.70; 60.25; 121.26; 123.10; 126.89; 138.01; 140.41; 141.82; 146.99; 172.90; 209.11. HR MS (ESI): 329.1865 (M+1), Calc. 329.1865.

*Sodium-(2R,S)-4-(2,4,6-triethylphenyl)-2-(1H-imidazole-1-yl)-4-oxobutanoate (**8a**)*

$C_{19}H_{23}N_2NaO_3$, starting from (2*R*,*S*)-4-(2,4,6-triethylphenyl)-2-(1*H*-imidazole-1-yl)-4-oxobutanoic acid (**8**) (0.000457 mol, 0.15 g) and an equimolar amount of NaOH (0.1 M), 0.094 g **8a** was obtained, 58.65 % yield, white solid. $^1$H NMR (200 MHz, $D_2O$) $\delta$ = 1.03 (*t*, 6H, *J*= 7.30 Hz, 2,6-$CH_2$–C$\underline{H}_3$); 1.17 (*t*, 3H, *J*= 7.86 Hz, 4-$CH_2$–C$\underline{H}_3$); 2.15-2.27 (*m*, 6H, 2,4,6-C$\underline{H}_2$–$CH_3$); 2.60 (*dd*, 1H, $J_{1,2}$= 7.30 Hz, $J_{1,3}$= 15.16 Hz); 3.65 (*d*, *br*, 1H, *J*= 7,30 Hz); 5.36 (*t*, *br*, 1H, *J*= 7.30 Hz); 7.05 (singlet like signal, 3H, 3,5-C$\underline{H}$–Ar and 4-C$\underline{H}$–imidazole); 7.22 (*s*, 1H, 5-C$\underline{H}$–imidazole); 7.78 (*s*, 1H, 2-C$\underline{H}$–imidazole). $^{13}$C NMR (50 MHz, $D_2O$) $\delta$ = 18.10; 28.00; 30.86; 32.94; 59.70; 122.22; 124.39; 128.14; 130.14; 139.77; 142.18; 148.11; 177.83; 212.80. IR ($\nu$, $cm^{-1}$): 1630.4 (Ar–C$\underline{(O)}$–), 1701.0 (–C$\underline{(O)}$–OH).

*(2R,S)-4-(4-Tertbutylphenyl)-2-(2-methyl-1H-imidazole-1-yl)-4-oxobutanoic acid (**9**)*

$C_{18}H_{22}N_2O_3$, starting from (*E*)-4-(4-*tert*-butylphenyl)-4-oxo-2-butenoic acid (0.00215 mol, 0.5 g) and 2-methyl-1*H*-imidazole (0.00258 mol, 0.212 g), 0.598 g of **9** was obtained, 88.46 % yield, white solid, m.p. 166 °C ($CH_2Cl_2$/$PhCH_3$). Insoluble in DMSO or $CHCl_3$, converted to sodium salt.

*Sodium-(2R,S)-4-(4-Tertbutylphenyl)-2-(2-methyl-1H-imidazole-1-yl)-4-oxobutano-ate (**9a**)*

$C_{18}H_{21}N_2NaO_3$, starting from (2 *R*,*S*)-4-(4-*tert*-butylphenyl)-2-(2-methyl-1*H*-imidazole-1-yl)-4-oxobutanoic acid (**9**) (0.00048 mol, 0.15 g) and an equimolar amount of NaOH (0.1 M), 0.102 g of **9a** was obtained, 63 % yield, white solid. $^1$H NMR (200 MHz, $D_2O$) $\delta$ = 1.08 (*s*, 9H, 4-(C$\underline{H}_3$)$_3$); 2.42 (*s*, *br*, 1H); 2.45 (*s*, 3H, imidazole-C$\underline{H}_3$); 3.75 (*d*, *br*, 1H, *J* = 9.55 Hz); 5.27 (triplet like signal, 1H, *J* = 5.62 Hz); 6.85 (*s*, *br*, 1H, 4-C$\underline{H}$–imidazole); 7.04 (*s*, *br*, 1H, 5-C$\underline{H}$–imidazole); 7.27 (*d*, 2H, *J* = 8.42 Hz, 2,6-C$\underline{H}$–Ar); 7.74 (*d*, 2H, *J* = 8.42 Hz, 3,5-C$\underline{H}$–Ar). $^{13}$C NMR (50 MHz, $D_2O$) $\delta$ = 14.46; 33.01; 37.14; 51.54; 59.26; 120.78; 123.66; 127.50; 128.23; 130.89; 135.84; 148.71; 160.18; 178.03; 201.31. IR ($\nu$, $cm^{-1}$): 1607.3 (Ar–C$\underline{(O)}$–), 1674.0 (–C$\underline{(O)}$–OH).

*(2R,S)-4-(3,4-Dimethylphenyl)-2-(2-methyl-1H-imidazole-1-yl)-4-oxobutanoic acid (**10**)*

$C_{16}H_{18}N_2O_3$, starting from (*E*)-4-(3,4-dimethylphenyl)-4-oxo-2-butenoic acid (0.00245 mol, 0.5 g) and 2-methyl-1*H*-imidazole (0.00294 mol, 0.241 g), 0.686 g **10** was obtained, 97.8 % yield, light yellow solid, m.p. 163 °C decomposition, ($CH_2Cl_2$/$PhCH_3$). Insoluble in DMSO or $CHCl_3$, converted to sodium salt.

*Sodium-(2R,S)-4-(3,4-dimethylphenyl)-2-(2-methyl-1H-imidazole-1-yl)-4-oxobuta-noate (**10a**)*

$C_{16}H_{17}N_2NaO_3$, starting from (2*R*,*S*)-4-(3,4-dimethylphenyl)-2-(2-methyl-1*H*-imidazole-1-yl)-4-oxobutanoic acid (**10**) (0.00052 mol, 0.15 g) and an equimolar amount of NaOH (0.1 M), 0.074 g **10a** was obtained, 45.8 % yield, light yellow solid.$^1$H NMR (200 MHz, $D_2O$) $\delta$ = 2.03 (doublet like signal, 6H, *J* = 6.18 Hz, 3,4-C$\underline{H}_3$–Ar); 2.5 (*s*, 3H, imidazole-C$\underline{H}_3$); 3.74–3.78 (*m*, 2H); 5.25 – 5.32 (*m*, 1H); 6.93–7.04 (*m*, 2H, 4,5-C$\underline{H}$–imidazole); 7.09 (*s*, 1H, 5-C$\underline{H}$–Ar); 7.44–7.49 (*d, br*, 2H, 2,6-C$\underline{H}$–Ar).$^{13}$C NMR (50 MHz, $D_2O$) $\delta$ = 17.64; 21.41; 21.78; 44.68; 61.14; 122.40; 123.32; 128.45; 131.40; 132.24; 135.95; 139.68; 140.07; 146.42; 177.77; 201.33. IR ($\nu$, $cm^{-1}$): 1619.0 (Ar–C$\underline{(O)}$–), 1674.8 (–C$\underline{(O)}$–OH).

*(2R,S)-4-(5,6,7,8-Tetrahydronaphtalene-2-yl)-2-(2-methyl-1H-imidazole-1-yl)-4-oxobutanoic acid (**11**)*

$C_{18}H_{20}N_2O_3$, starting from (*E*)-4-(5,6,7,8-tetrahydronaphtalene-2-yl)-4-oxo-2-butenoic acid (0.00217 mol, 0.5 g) and 2-methyl-1*H*-imidazole (0.0026 mol, 0.213 g), 0.668 g of **11** was obtained, 98.52 % yield, light brown solid, m.p. 161 °C, ($CH_2Cl_2$/$PhCH_3$). Insoluble in DMSO or $CHCl_3$, converted to sodium salt.

*Sodium-(2R,S)-4-(5,6,7,8-tetrahydronaphtalene-2-yl)-2-(2-methyl-1H-imidazole-1-yl)-4-oxobutanoate (**11a**)*

$C_{18}H_{19}N_2NaO_3$, starting from (2*R*,*S*)-4-(5,6,7,8-tetrahydronaphtalene-2-yl)-2-(2-methyl-1*H*-imidazole-1-yl)-4-oxobutanoic acid **(11)** (0,00048 mol, 0,15 g) and an equimolar amount of NaOH (0.1 M), 0.102 g **11a** was obtained, 63.5 % yield, brown solid. $^1$H NMR (200 MHz, $D_2O$) $\delta$: 1.51 (*s*, *b*, 2H, 3,4-($CH_2$–C$\underline{H}_2$)–); 2.47–2.52 (*d*, *b*, 3H, 3,4-(C$\underline{H}_2$–$CH_2$)–); 2.58 (*s*, 3H, imidazole-C$\underline{H}_3$); 3.81–3.86 (*d*, *b*, 1H, *J* = 10.11 Hz); 5.37 (*t*, *b*, 1H, *J* = 5.05 Hz); 6.84–6.88 (*d*, 1H, *J* = 7.86 Hz, 4-C$\underline{H}$–imidazole); 6.95 (*s*, 1H, 5-C$\underline{H}$–Ar); 7.10–7.13 (*d*, 1H, *J* = 6.18 Hz, 5-C$\underline{H}$–imidazole); 7.46 (*s*, 1H, 2-C$\underline{H}$–Ar); 7.52–7.56 (*d*, 1H, *J* = 8.42 Hz, 6-C$\underline{H}$–Ar). $^{13}$C NMR (50 MHz, $D_2O$) $\delta$: 14.60; 14.98; 25.05; 31.24; 31.68; 120.40; 123.70; 127.83; 131.29; 131.71; 135.84; 139.65; 146.02; 148.73; 178.26; 200.86. IR ($\nu$, $cm^{-1}$): 1609.2 (Ar–C$\underline{(O)}$–), 1679.4 (–C$\underline{(O)}$–OH).

*(2R,S)-4-(2,4,6-Triethylphenyl)-2-(2-methyl-1H-imidazole-1-yl)-4-oxobutanoic acid (**12**)*

$C_{20}H_{26}N_2O_3$, starting from (*E*)-4-(2,4,6-triethylphenyl)-4-oxo-2-butenoic acid (0.00192 mol, 0.5 g) and 2-methyl-1*H*-imidazole (0.0023 mol, 0.189 g), 0.582 g of **12** was obtained, 88.58 % yield, light yellow solid, m.p. 165 °C ($CH_2Cl_2$/$PhCH_3$). $^1$H NMR (200 MHz, $CDCl_3$) $\delta$: 1.11 (*t*, 6H, *J* = 7.86 Hz, 2,6-$CH_2$–C<u>H</u>$_3$); 1.22 (*t*, 3H, *J* = 7.30 Hz, 4-$CH_2$–C<u>H</u>$_3$); 2.28 (*q*, 4H, $J_{1,2}$ = 7.86 Hz, $J_{1,3}$ = 15.16 Hz, 2,6-C<u>H</u>$_2$–$CH_3$); 2.38 (*s*, 3H, imidazole-C<u>H</u>$_3$); 2.60 (*q*, 2H, $J_{1,2}$ = 7.86 Hz, $J_{1,3}$ = 15.16 Hz, 4-C<u>H</u>$_2$–$CH_3$); 3.47 (dd, 1H, $J_{1,2}$ = 8.99 Hz, $J_{1,3}$ = 19.09 Hz); 3.90 (*dd*, 1H, $J_{1,2}$ = 16.85 Hz, $J_{1,3}$ = 19.66 Hz); 5.39 (*dd*, 1H, $J_{1,2}$ = 7.86 Hz, $J_{1,3}$ = 10.67 Hz); 6.88 (*s*, 2H, 3-C<u>H</u>–Ar); 7.16 (*dd*, 1H, $J_{1,2}$ = 6.74 Hz, $J_{1,3}$ = 8.99 Hz, 5-C<u>H</u>–imidazole). $^{13}$C NMR (50 MHz, $CDCl_3$) $\delta$: 11.38; 15.37; 15.82; 25.95; 28.68; 48.65; 56.86; 118.89; 119.40; 125.74; 137.15; 138.94; 144.95; 145.53; 171.38; 207.00. HR MS (ESI): 343.1951 (M+1), Calc. 343.2022; 341.1915 (M+1), Calc. 341.1865.

*Sodium-(2R,S)-4-(2,4,6-triethylphenyl)-2-(2-methyl-1H-imidazole-1-yl)-4-oxobutanoate (**12a**)*

$C_{20}H_{25}N_2NaO_3$, starting from (2*R*,*S*)-4-(2,4,6-triethylphenyl)-2-(2-methyl-1*H*-imidazole-1-yl)-4-oxobutanoic acid **(12)** (0.00044 mol, 0.15 g) and an equimolar amount of NaOH (0.1 M), 0.095 g of **12a** was obtained, 59.3% yield, light yellow solid. $^1$H NMR (200 MHz, $D_2O$) $\delta$: 0.87–1.03 (*m*, 9H, 2,4,6-$CH_2$–C<u>H</u>$_3$); 2.10 (*d*, *b*, 4H, *J*= 7.30 Hz, 2,6-C<u>H</u>$_2$–$CH_3$); 2.36 (*d*, *b*, 1H, *J*= 7.86 Hz); 2.42 (*d*, 3H, *J*= 7.30 Hz, 4-C<u>H</u>$_2$–$CH_3$); 3.38 (*s*, 1H, imidazole-C<u>H</u>$_3$); 5.31 (*s*, *b*, 1H); 6.75 (*s*, 2H, 3,5-C<u>H</u>–Ar); 6.94 (*s*, 1H, 4-C<u>H</u>–imidazole); 7.02 (*d*, 1H, *J*= 8.99 Hz, 5-C<u>H</u>–imidazole). $^{13}$C NMR (50 MHz, $D_2O$) $\delta$: 14.51; 17.57; 18.08; 28.08; 30.84; 51.58; 58.43; 121.42; 123.66; 128.16; 139.74; 142.16; 148.06; 148.84; 177.63; 212.58. IR ($\nu$, $cm^{-1}$): 1614.5 (Ar–<u>C(O)</u>–), 1700.4 (-<u>C(O)</u> -OH).

*(2R,S)-4-(4-Fluorophenyl)-2-(1H-indole-3-yl)-4-oxobutanoic acid (**13**)*

$C_{18}H_{14}FNO_3$, starting from (*E*)-4-(4-fluorophenyl)-4-oxo-2-butenoic acid (0.0022 mol, 0.426 g) and 1*H*-indole (0.00264 mol, 0.309 g), 0.205 g of **13** was obtained, 29.93 % yield, light brown solid, m.p. 162 °C decomposition, ($CH_2Cl_2$/$PhCH_3$). $^1$H NMR (200 MHz, DMSO-$d_6$) $\delta$: 3.29 (*d*, *b*, 1H, *J*= 3.37 Hz); 4.00 (*dd*, 1H, $J_{1,2}$ = 7.30 Hz, $J_{1,3}$ = 17.97 Hz); 4.34 (*dd*, 1H, $J_{1,2}$ = 6.74 Hz, $J_{1,3}$ = 10.67 Hz); 6.97–7.13 (*m*, 2H, 3,5-C<u>H</u>–Ar); 7.31-7.40 (*m*, 4H, 2,5,6,7-C<u>H</u>–indole); 7.70 (*d*, 1H, *J*= 7.30 Hz, 4-C<u>H</u>–indole); 8.13 (*dd*, 2H, $J_{1,2}$ = 3.37 Hz, $J_{1,3}$ = 8.99 Hz, 2,6-C<u>H</u>–Ar); 11.03 (*s*, 1H, N-<u>H</u>); 12.20 (*s*, 1H, -C(O)-O<u>H</u>). $^{13}$C NMR (50 MHz, DMSO-$d_6$) $\delta$: 37.86; 41.34; 111.76; 112.12; 115.77; 116.20; 118.88; 119.32; 121.43; 123.52; 126.49; 131.19; 131.39; 136.50; 162.87; 167.87; 174.99; 197.35. IR ($\nu$, $cm^{-1}$): 1679.0 (Ar–<u>C(O)</u>–), 1716.0 (–<u>C(O)</u>–OH), 3416.7 ($R_2$<u>NH</u>). HR MS (ESI): 312.0862 (M+1), Calc. 312.1036; 310.0940 (M–1), Calc. 310.0879.

*(2R,S)-4-(4-Ethylphenyl)-2-(1H-indole-3-yl)-4-oxobutanoic acid (**14**)*

$C_{20}H_{19}NO_3$, starting from (*E*)-4-(4-ethylphenyl)-4-oxo-2-butenoic acid (0.00192 mol, 0.5 g) and 1*H*-indole (0.0023 mol, 0.269 g), 0.142 g **14** was obtained, 19.64 % yield, dark yellow solid, m.p. 159 °C decomposition, ($CH_2Cl_2$/$PhCH_3$). $^1$H NMR (200 MHz, DMSO-$d_6$) $\delta$: 1.20 (*t*, 3H, *J*= 7.86 Hz, 4-$CH_2$–C<u>H</u>$_3$); 2.68 (*dd*, 2H, $J_{1,2}$ = 7.30 Hz, $J_{1,3}$ = 15.16 Hz, 4-C<u>H</u>$_2$–$CH_3$); 3.27 (*d*, *b*, 1H, *J*= 3.93 Hz); 4.00 (*dd*, 1H, $J_{1,2}$ = 7.30 Hz, $J_{1,3}$ = 17.97 Hz); 4.35 (*dd*, 1H, $J_{1,2}$ = 6.74 Hz, $J_{1,3}$ = 10.11 Hz); 6.98–7.14 (*m*, 2H, 2,6-C<u>H</u>–Ar); 7.34–7.39 (*m*, 4H, 3,5-C<u>H</u>–Ar and 5,6-C<u>H</u>–indole); 7.70 (*d*, 1H, *J*= 7.30 Hz, 2-C<u>H</u>–indole); 7.97 (*d*, 2H, *J*= 7.86 Hz, 4,7-C<u>H</u>–indole); 11.03 (*s*, 1H, N<u>H</u>); 12.20 (*s*, 1H, -C(O)-O<u>H</u>). $^{13}$C NMR(50*MHz*, *DMSO*) $\delta$: 15.45; 28.41; 37.86; 41.26; 111.76; 112.22; 118.86; 119.28; 121.39; 123.47; 126.49; 128.35; 128.46; 134.48; 136.50; 149.94; 175.03; 198.17. IR ($\nu$, $cm^{-1}$): 1673.0 (Ar–<u>C(O)</u>–), 1726.7 (–<u>C(O)</u>–OH), 3395.8 ($R_2$<u>NH</u>). HR MS (ESI): 322.1273 (M+1), Calc. 322.2069; 320.1347 (M–1), Calc. 320.1287.

*(2R,S)-4-(4-Isopropylphenyl)-2-(1H-indole-3-yl)-4-oxobutanoic acid (**15**)*

$C_{21}H_{21}NO_3$, starting from (*E*)-4-(4-isopropylphenyl)-4-oxo-2-butenoic acid (0.0023 mol, 0.5 g) and 1*H*-indole (0.00275 mol, 0.322 g), 0.2 g **15** was obtained, 25.93 % yield, light brown solid, m.p. 104 °C decomposition, ($PhCH_3$). $^1$H NMR (200 MHz, DMSO-$d_6$) $\delta$: 1.22 (*d*, 6H, *J*= 6.74 Hz, 4-CH-(C<u>H</u>$_3$)$_2$); 2.97 (*qv*, 2H, $J_{1,2}$ = 6.74 Hz, $J_{1,3}$ = 14.04 Hz, 4-C<u>H</u>-($CH_3$)$_2$); 3.27 (*d*, *b*, 1H, *J*= 3.93 Hz); 4.02 (*dd*, 1H, $J_{1,2}$ = 7.30 Hz, $J_{1,3}$ = 17.97 Hz); 4.35 (*dd*, 1H, $J_{1,2}$ = 6.74 Hz, $J_{1,3}$ = 10.11 Hz); 6.98–7.14 (*m*, 2H, 2,6-C<u>H</u>–Ar); 7.36–7.42 (*m*, 4H, 2,5,6,7-C<u>H</u>–indole); 7.69 (*d*, 1H, *J*= 7.30 Hz, 4-C<u>H</u>–indole); 7.97 (*d*, 2H, *J*= 8.42 Hz, 3,5-C<u>H</u>–Ar); 11.02 (*s*, 1H, *N*-<u>H</u>); 12.17 (*s*, 1H, –COO<u>H</u>). $^{13}$C NMR (50 MHz, DMSO-$d_6$) $\delta$: 23.73; 33.73; 37.86; 41.25; 111.76; 112.22; 118.86; 119.28; 121.39; 123.45; 126.49; 126.89; 128.49; 134.65; 136.50; 154.42; 175.01; 198.15. IR ($\nu$, $cm^{-1}$): 1606.8 (Ar–<u>C(O)</u>–), 1668.7 (–<u>C(O)</u>–OH), 3350.3 ($R_2$<u>NH</u>). HR MS (ESI): 336.1406 (M+1), Calc. 336.1600; 334.1494 (M–1), Calc. 334.1443.

*(2R,S)-4-(4-Tertbutylphenyl)-2-(1H -indole-3-yl)-4-oxobutanoic acid (**16**)*

$C_{22}H_{23}NO_3$, starting from (*E*)-4-(4-*tert*-butylphenyl)-4-oxo-2-butenoic acid (0.00215 mol, 0.5 g) and 1*H*-indole (0.00258 mol, 0.302 g), 0.464 g of **16** was obtained, 61.78 % yield, dark yellow solid, m.p. 107 °C decomposition, (petroleum-ether/$Et_2O$). Crude product was recrystallized using petroleum-ether/$Et_2O$ mixture. Precipitate was rinsed with petroleum-ether. $^1$H NMR (200 MHz, DMSO-$d_6$) $\delta$: 1.31 (*s*, 9H, 4-C(C$\underline{H}_3$)$_3$); 3.36 (*dd*, 1H, $J_{1,2}$ = 13.48 Hz, $J_{1,3}$ = 17.97 Hz); 3.97 (*dd*, 1H, $J_{1,2}$ = 7.86 Hz, $J_{1,3}$ = 17.97 Hz); 4.60 (*dd*, 1H, $J_{1,2}$ = 5.62 Hz, $J_{1,3}$ = 9.55 Hz); 7.07–7.34 (*m*, 3H, 2,6-C$\underline{H}$–Ar and 2-C$\underline{H}$–indole); 7.42 (*d*, 2H, *J*= 8,42 Hz, 5,6-C$\underline{H}$–indole); 7.72 (*d*, 1H, *J*= 7.30 Hz, 7-C$\underline{H}$–indole); 7.88 (*d*, 2H, *J*= 8.42 Hz, 3,5-C$\underline{H}$–Ar); 8.15 (*d*, 1H, *J*= 1.68 Hz, 4-CH–indole). $^{13}$C NMR (50 MHz, DMSO-$d_6$)$\delta$: 31.03; 35.09; 37.74; 41.44; 95.77; 111.43; 112.34; 119.20; 119.88; 122.37; 122.64; 125.56; 128.12; 133.82; 136.24; 157.09; 179.01; 197.82. IR $\nu$, cm$^{-1}$): 1669.0 (Ar–$\underline{C(O)}$–), 1718.2 (–$\underline{C(O)}$–OH), 3326.2 (R$_2\underline{NH}$). HR MS (ESI): 350.1548 (M+1), Calc. 350.1756; 348.1652 (M–1), Calc. 348.1600.

*(2R,S)-4-(2,4-Dimethylphenyl)-2-(1H-indole-3-yl)-4-oxobutanoic acid (**17**)*

$C_{20}H_{19}NO_3$, starting from (*E*)-4-(2,4-dimethylphenyl)-4-oxo-2-butenoic acid (0.00206 mol, 0.42 g) and 1*H*-indole (0.00246 mol, 0.288 g), 0.378 g **17** was obtained, 57.1 % yield, dark yellow solid, m.p. 162 °C decomposition, ($CH_2Cl_2$/$PhCH_3$). $^1$H NMR (500 MHz, DMSO-$d_6$) $\delta$: 2.31 (*s*, 3H, 4-C$\underline{H}_3$–Ar); 2.37 (*s*, 3H, 2-C$\underline{H}_3$–Ar); 3.23 (*dd*, 1H, $J_{1,2}$ = 13.51 Hz, $J_{1,3}$ = 17.87 Hz); 3.88 (*dd*, 1H, $J_{1,2}$ = 6.98 Hz, $J_{1,3}$ = 17.44 Hz); 4.32 (*dd*, 1H, $J_{1,2}$ = 6.54 Hz, $J_{1,3}$ = 10.46 Hz); 7.00 (*d*, 1H, *J*= 7.85 Hz, 5-C$\underline{H}$–indole); 7.09 (*d*, 1H, *J*= 2.62 Hz, 6-C$\underline{H}$–indole); 7.10 (*t*, 1H, *J*= 6,98 Hz, 3-C$\underline{H}$–Ar); 7.11–7.13 (*d*, 1H, *J*= 7,85 Hz, 5-C$\underline{H}$–Ar); 7.30 (*s*, 1H, 2-C$\underline{H}$–indole); 7.36 (*d*, 1H, *J*= 7.85 Hz, 4-C$\underline{H}$–indole); 7.65 (*d*, 1H, *J*= 2.62 Hz, 7-C$\underline{H}$–indole); 7.79 (*d*, 1H, *J*= 7.85 Hz, 6-C$\underline{H}$–Ar); 11.00 (*s*, 1H, N$\underline{H}$); 12.21 (*s*, 1H, –COO$\underline{H}$). $^{13}$C NMR (125 MHz, DMSO-$d_6$) $\delta$: 20.85; 20.89; 38.05; 43.71; 111.51; 111.85; 118.60; 118.97; 121.14; 123.19; 126.21; 126.41; 129.23; 132.33; 134.71; 136.24; 137.40; 141.41; 174.79; 201.69. IR ($\nu$, cm$^{-1}$): 1668.9 (Ar–$\underline{C(O)}$–), 1707.0 (–$\underline{C(O)}$–OH), 3426.8 (R$_2\underline{NH}$). HR MS (ESI): 322.1273 (M+1), Calc. 322.1443; 320.1337 (M–1), Calc. 320.1287.

*(2R,S)-4-(2,5-Dimethylphenyl)-2-(1H-indole-3-yl)-4-oxobutanoic acid (**18**)*

$C_{20}H_{19}NO_3$, starting from (*E*)-4-(2,5-dimethylphenyl)-4-oxo-2-butenoic acid (0.00245 mol, 0.5 g) and 1*H*-indole (0.00294 mol, 0.344 g), 0.627 g of **18** was obtained, 79.67 % yield, light brown solid, m.p. 164 °C ($CH_2Cl_2$/$PhCH_3$). $^1$H NMR (200 MHz, DMSO-$d_6$) $\delta$: 2.32 (*d*, 6H, *J*= 2.25 Hz, 2,5-C$\underline{H}_3$–Ar); 3.25 (*dd*, 1H, $J_{1,2}$ = 13.48 Hz, $J_{1,3}$ = 17.97 Hz); 3.86 (*dd*, 1H, $J_{1,2}$ = 7.30 Hz, $J_{1,3}$ = 17.97 Hz); 4.31 (*dd*, 1H, $J_{1,2}$ = 6.74 Hz, $J_{1,3}$ = 10.67 Hz); 6.97–7.26 (*m*, 4H, 2,5,6-C$\underline{H}$–indole and 3-C$\underline{H}$–Ar); 7.32–7.39 (*m*, 2H, 4-C$\underline{H}$–Ar and 7-C$\underline{H}$–indole); 7.66 (*s*, *b*, 2H, 6-C$\underline{H}$–Ar and 4-C$\underline{H}$–indole); 11.02 (*s*, 1H, N$\underline{H}$); 12.23 (*s*, 1H, –COO$\underline{H}$). $^{13}$C NMR (50 MHz, DMSO-$d_6$) $\delta$: 20.38; 20.62; 38.19; 44.18; 111.76; 112.03; 118.86; 119.23; 121.39; 123.49; 126.45; 129.37; 131.74; 132.10; 134.05; 135.27; 136.49; 137.83; 175.07; 202.83. IR ($\nu$, cm$^{-1}$): 1566.4 (Ar–$\underline{C(O)}$–), 1692.9 (–$\underline{C(O)}$–OH), 3414.1 (R$_2\underline{NH}$). HR MS (ESI): 322.1155 (M+1), Calc. 322.1443; 320.1343 (M–1), Calc. 320.1287.

*(2R,S)-4-(3,4-Dimethylphenyl)-2-(1H-indole-3-yl)-4-oxobutanoic acid (**19**)*

$C_{20}H_{19}NO_3$, starting from (*E*)-4-(3,4-dimethylphenyl)-4-oxo-2-butenoic acid (0.00245 mol, 0.5 g) and 1*H*-indole (0.00294 mol, 0.344 g), 0.303 g of **19** was obtained, 38.5 % yield, dark yellow solid, m.p. 164 °C decomposition, ($CH_2Cl_2$/$PhCH_3$). $^1$H NMR (200 MHz, $CD_3OD$)$\delta$: 2.29 (*s*, 6H, 3,4-C$\underline{H}_3$–Ar); 3.34 (*d*, *b*, 1H, *J*= 3,93 Hz); 3.99 (*dd*, 1H, $J_{1,2}$ = 7.30 Hz, $J_{1,3}$ = 17.97 Hz); 4.33 (*dd*, 1H, $J_{1,2}$ = 6.74 Hz, $J_{1,3}$ = 10.67 Hz); 6.97 – 7.13 (*m*, 2H, 2,6-C$\underline{H}$–Ar); 7.27–7.39 (*m*, 3H, 2,5,6-C$\underline{H}$–indole); 7.66–7.82 (*m*, 3H, 4,7-C$\underline{H}$–indole and 5-C$\underline{H}$–Ar); 11.02 (*s*, 1H, N$\underline{H}$); 12.16 (*s*, 1H, –COO$\underline{H}$). $^{13}$C NMR (50 MHz, $CD_3OD$) $\delta$: 19.51; 19.80; 37.86; 41.28; 111.74; 112.25; 118.84; 119.30; 121.39; 123.47; 125.87; 126.49; 129.22; 129.99; 134.63; 136.50; 136.98; 142.66; 175.05; 198.30. IR ($\nu$, cm$^{-1}$): 1668.4 (Ar–$\underline{C(O)}$–), 1714.4 (–$\underline{C(O)}$–OH), 3344.4 (R$_2\underline{NH}$). HR MS (ESI): 322.1436 (M+1), Calc. 322.1443.

*(2R,S)-4-(2,4-Diisopropylphenyl)-2-(1H-indole-3-yl)-4-oxobutanoic acid (**20**)*

$C_{24}H_{27}NO_3$, starting from (*E*)-4-(2,4-diisopropylphenyl)-4-oxo-2-butenoic acid (0.002 mol, 0.5 g) and 1*H*-indole (0.0024 mol, 0.281 g), 0.257 g **20** was obtained, 34.04 % yield, dark brown resin.$^1$H NMR (200 MHz, DMSO-$d_6$) $\delta$: 1.13 (*s*, 6H, 2-CH(C$\underline{H}_3$)$_2$); 1.19 (*s*, 6H, 4-CH(C$\underline{H}_3$)$_2$); 2.92 (*qv*, 1H, $J_{1,2}$ = 7.30 Hz, $J_{1,3}$ = 14.04 Hz); 3.19–3.43 (*m*, 4H, 2,4-C$\underline{H}$(CH$_3$)$_2$); 3.82 (*dd*, 1H, $J_{1,2}$ = 7.30 Hz, $J_{1,3}$ = 17.97 Hz); 4.34 (*dd*, 1H, $J_{1,2}$ = 6.18 Hz, $J_{1,3}$ = 10.67 Hz); 6.99–7.17 (*m*, 3H, 5-C$\underline{H}$–Ar and 5,6-C$\underline{H}$–indole); 7.30–7.38 (*m*, 3H, 3-C$\underline{H}$–Ar and 4,7-C$\underline{H}$–indole); 7.63 (*t*, 2H, *J*= 7.30 Hz, 2-C$\underline{H}$–indole and 6-C$\underline{H}$–Ar); 11.01 (*s*, 1H, N$\underline{H}$); 12.26 (*s*, 1H, –COO$\underline{H}$). $^{13}$C NMR (50 MHz, DMSO-$d_6$) $\delta$: 23.88; 24.22; 28.68; 33.76; 45.07; 65.15; 111.76; 111.94; 118.84; 119.19; 120.23; 121.37; 123.49; 124.54; 128.07; 136.50; 147.41; 151.72; 175.03; 204.03. IR ($\nu$, cm$^{-1}$): 1605.9 (Ar–

C(O)–), 1690.3 (–C(O)–OH), 3382.6 ($R_2$NH). HR MS (ESI): 378.2081 (M+1), Calc. 378.2069.

*(2R,S)-4-(2,4,6-Triethylphenyl)-2-(1H-indole-3-yl)-4-oxobutanoic acid (**21**)*

$C_{24}H_{27}NO_3$, starting from (*E*)-4–(2,4,6-triethylphenyl)-4-oxo-2-butenoic acid (0.00192 mol, 0.5 g) and 1*H*-indole (0.0023 mol, 0.269 g), 0.142 g of **21** was obtained, 19.64 % yield, light brown solid, m.p. 136 °C decomposition, (petroleum-ether/ $Et_2O$). Crude product was recrystalized from petroleum-ether/$Et_2O$ mixture, then rinsed with petroleum-ether on the funnel. $^1$H NMR (200 MHz, $CDCl_3$) $\delta$: 1.11 (*t*, 6H, *J*= 7.30 Hz, 2,6-$CH_2$–C$H_3$); 1.21 (*t*, 3H, *J*= 7.86 Hz, 4-$CH_2$–C$H_3$); 2.41 (*dd*, 4H, $J_{1,2}$ = 7.30 Hz, $J_{1,3}$ = 15.16 Hz, 2,6-C$H_2$–$CH_3$); 2.60 (*dd*, 2H, $J_{1,2}$ = 7.86 Hz, $J_{1,3}$ = 15.16 Hz, 4-C$H_2$–$CH_3$); 3.19 (*dd*, 1H, $J_{1,2}$ = 15.16 Hz, $J_{1,3}$ = 19.66 Hz); 3.76 (*dd*, 1H, $J_{1,2}$ = 9.55 Hz, $J_{1,3}$ = 19.09 Hz); 4.60 (*dd*, 1H, $J_{1,2}$ = 5.62 Hz, $J_{1,3}$ = 9.55 Hz); 6.87 (*s*, *b*, 2H, 5,6-CH–indole); 7.12–7.26 (*m*, 2H, 3,5-CH–Ar); 7.34 (*d*, 1H, *J*= 7.30 Hz, 2-CH–indole); 7.72 (*d*, 1H, *J*= 7.86 Hz, 7-CH–indole); 8.13 (*s*, 1H, 4-CH–indole). $^{13}$C NMR (50 MHz, $CDCl_3$) $\delta$: 15.42; 15.90; 25.84; 28.66; 37.11; 48.20; 111.30; 112.12; 119.24; 119.97; 122.46; 122.55; 125.59; 136.15; 139.28; 145.11; 178.74; 208.42. IR ( $\nu$, $cm^{-1}$): 1611.4 (Ar–C(O)–), 1700.1 (–C(O)–OH), 3451.0 ($R_2$NH). HR MS (ESI): 378.1862 (M+1), Calc. 378.2069; 376.1973 (M–1), Calc. 376.1913.

## Biological assays

### Cytotoxicity assays

*Preparation of compound solutions*

Stock solutions of the investigated compounds were made in dimethyl sulfoxide (Fluka, Switzerland) or in distilled water at concentration of 20 mM, filtered through Millipore filters (0.22 μm) before use and afterwards diluted to various working concentrations with RPMI-1640 cell culture medium (Sigma Chemical Co. St Louis, MO) supplemented with 3 mmol/L L-glutamine, 200 μg/mL streptomycin, 192 IU/mL penicillin, 10 % heat inactivated fetal bovine serum (FBS, Sigma Chemical Co.), and 25 mM Hepes, adjusted to pH 7.2 with a bicarbonate solution.

*Treatment of cells*

Cells were seeded into 96-well microtiter plates, 2000 cells in 0.1 mL of culture medium per well for HeLa cells, 7000 cells/well for LS174 and MDA-MB-361, and 5000 cells/well for K562 and FemX cells. After 24 h, to wells with the cells, five different concentrations of compounds **1**–**21** were applied, except to the control wells, in which cells were grown in medium only. All concentrations were set up in triplicate. Culture medium with corresponding concentrations of investigated compounds, but without cells, was used as a blank, also in triplicate.

*Preparation of Peripheral Blood Mononuclear cells, PBMC*

PBMC were separated from whole heparinized blood of three healthy volunteers by Lymphoprep gradient centrifugation. Interface cells, washed three times with Haemaccel (aqueous solution supplemented with 145 mM $Na^+$, 5. 1 mM $K^+$, 6. 2 mM $Ca^{2+}$, 145 mM $Cl^-$, and 35 g/L gelatin polymers, pH 7.4), were counted and resuspended in nutrient medium.

*Treatment of PBMC*

PBMC were seeded (150000 cells per well) into nutrient medium, or in nutrient medium enriched with 5 μg/mL phytohaemaglutinin (PHA) (Welcome) in 96-well microtiter plates, and 2 h later, investigated compounds were added to the wells, in triplicate, to five final concentrations, except to the control wells, where a nutrient medium only was added to the cells. Nutrient medium with corresponding concentrations of compounds, but void of cells, was used as a blank.

*Determination of cell survival*

Cell survival was determined by the MTT test, according to the method of Mosmann [19] as modified by Ohno and Abe [20], 72 h after treatment with the investigated compounds. Briefly, 10 μL of MTT solution (5 mg/mL in phosphate buffered saline) was added to each well. Cells were incubated for 4 h at 37 °C in a humidified atmosphere with 5 % $CO_2$. Then, 100 μL of 10% SDS was added to each well. Absorbance was measured at 570 nm. Cell survival was measured/quantified using absorbance at 570 nm of a sample with cells grown in the presence of various concentrations of the compounds, divided by the absorbance of the control sample (the absorbance of cells grown in nutrient medium only). Absorbance of blank was always subtracted from absorbance of a corresponding sample with cells. All experimentally obtained $IC_{50}$ data, reported in Table 2, are means of at least three measurements done in triplicate.

### Determination of the type of cell death

The type of cell death was determined by AO/EB (acridine orange/ethidium bromide) staining method. HeLa cells were seeded overnight on coverslips (30,000 cells) in 2 ml of complete medium. After 24 h, compounds were added in concentrations that caused the death of 90 % of cells ($IC_{90}$) and cells

were incubated with compounds for 24 h. $IC_{90}$ values were determined from dose-response curves separately. After this period, coverslips with target cells were stained with acridine orange/ethidium bromide mixture (3 μg/ml AO and 10 μg/ml EB in PBS), and visualized under a fluorescence microscope. Additionally, supernatant from Petri dishes in which cells were incubated with compounds was centrifuged and precipitate mixed with AO/EB. Such suspension was also applied on microscope coverslips and visualized under fluorescence microscope.

### Cell cycle determination

Aliquots of $2.5 \times 10^5$ control cells, or cells treated with concentrations that correspond to $IC_{50}$ value of the investigated compounds for 24 h, were fixed in 70 % ethanol for 1 h on ice, then at −20°C for at least 1 week. The cells were then collected by centrifugation. The pellets were treated with RNase (100 μg/mL) at 37 °C for 30 min and then incubated with propidium iodide (40 μg/mL) for at least 30 min. DNA content and cell cycle distribution were analyzed using a Becton Dickinson FAC-Scan flow cytometer. Flow cytometric analysis was performed using a CellQuestR (Becton Dickinson, San Jose, CA, USA) on a minimum of 10,000 cells per sample [21].

### Molecular modeling

3D structures of compounds under study (**1**–**21**) were generated in OMEGA [22–24] from SMILES notation. MMFF94s force field [25] was used. SMILES notations of compounds in ionization states estimated on pH 7 are given in Table S1 in Supplementary material. Conformation perceived as global minimum for each compound was saved in mol2 format and used in further calculations. Arbitrarily, the (*S*)-configuration was ascribed to the stereogenic center for all compounds. 3D QSAR models were built by using alignment-independent descriptors GRIND-2, derived from molecular interaction fields, as applied in Pentacle 1.0.6 program [17]. Discretization of MIF was done using AMANDA algorithm [18]. CLACC algorithm was used for alignment of molecules. GRID resolution was set to 0.4 Å, and DRY (hydrophobic), N1 (HBD), O (HBA), and TIP (shape) probes were used. Protonation states of molecules at pH 7.0 were ascribed automatically by the program. In this way, the –COOH group was perceived in its anionic state ($–COO^-$) for all molecules, while the N4 atom in *N*-Me-piperazine derivatives was protonated. For modeling purposes, experimentally obtained $IC_{50}$ values in molar concentrations (M) were converted to corresponding negative decade logarithms, $p(IC_{50})$. Virtual log *P* values [26] of molecules in neutral form were calculated from the 3D structures of compounds, obtained as the global minima from OMEGA, in VegaZZ 3.0.1 [27].

**Acknowledgments** This work is supported by the Ministry of Education, Science and Technological Development of Serbia, under Grant 172035. Authors gratefully acknowledge OpenEye Scientific Software, Santa Fe, NM, for the free academic licensing of software tools.

## References

1. Bougault J (1908) Sur l'acide benzoylacrylique. Ann Chim Phys 15:491–515
2. Cromwell NH, Creger PL, Cook KE (1956) Studies with the amine adducts of *para*-benzoylacrylic acid and its methyl ester. J Am Chem Soc 78:4412–4415. doi:10.1021/ja01598a058
3. Li X, Liu N, Zhang H, Knudson SE, Li H-J, Lai C-T, Simmerling C, Slayden RA, Tonge PJ (2011) CoA adducts of 4-oxo-4-phenylbut-2-enoates: inhibitors of MenB from the *M. tuberculosis* menaquinone biosynthesis pathway. ACS Med Chem Lett 2:818–823. doi:10.1021/ml200141e
4. Hayashi K, Neve J, Hirose M, Kuboki A, Shimada Y, Kepinski S, Nozaki H (2012) Rational design of an auxin antagonist of the $SCF^{TIR1}$ auxin receptor complex. ACS Chem Biol 7:590–598. doi:10.1021/cb200404c
5. PubChem's BioAssay, AID 376: HTS Discovery of chemical inhibitors of HePTP, a leukemia target. Burnham Center for Chemical Genomics
6. Wang Y, Xiao J, Suzek TO, Zhang J, Wang J, Zhou Z, Han L, Karapetyan K, Dracheva S, Shoemaker BA, Bolton E, Gindulyte A, Bryant SH (2012) PubChem's BioAssay database. Nucleic Acids Res 40:D400–D412. doi:10.1093/nar/gkr1132
7. Couquelet J, Couquelet J, Cluzel R, Tronche P (1969) Antibacterial α-amino-β-aroylpropionic acids. Chim Ther 4:127–130
8. Gieldanowski J, Steuden W (1981) Screening system for the evaluation of preparations with potential cytostatic and immunotropic activity. II. Derivatives of propionic and hydroxybutyric acids and of tetrahydrofuran-2-one. Arch Immunol Ther Exp 29:257–265
9. Drakulić BJ, Stanojković TP, Žižak ŽS, Dabović MM (2011) Antiproliferative activity of aroylacrylic acids. Structure–activity study based on molecular interaction fields. Eur J Med Chem 46:3265–3273. doi:10.1016/j.ejmech.2011.04.043
10. Drakulić BJ, Juranić ZD, Stanojković TP, Juranić IO (2005) 2-[(Carboxymethyl) sulfanyl]-4-oxo-4-arylbutanoic acids selectively suppressed proliferation of neoplastic human HeLa cells. A SAR/QSAR study. J Med Chem 48:5600–5603. doi:10.1021/jm0502889
11. Vitorović-Todorović MD, Erić-Nikolić A, Kolundžija B, Hamel E, Ristić S, Juranić IO, Drakulić BJ (2013) (*E*)-4-Aryl-4-oxo-2-butenoic acid amides, chalcone-aroylacrylic acid chimeras: design, antiproliferative activity and inhibition of tubulin polymerization. Eur J Med Chem 62:40–50. doi:10.1016/j.ejmech.2013.01.006
12. Papa D, Schwenk E, Villani F, Klingsberg E (1948) β-Aroylacrylic acids. J Am Chem Soc 70:3356–3360. doi:10.1021/ja01190a041
13. Abubshait SA (2007) An efficient synthesis and reactions of novel indolylpyridazinone derivatives with expected biological activity. Molecules 12:25–42. doi:10.3390/12010025
14. Tamam GH, Soliman EA, El-Gendy AM, Al-Kady AY (1987) Alkylation of indole with β-aroylacrylic acids and some studies on the alkylated products. J Chem Soc Pak 9:1–10
15. Goodford PJ (1985) A computational procedure for determining energetically favorable binding sites on biologically important macromolecules. J Med Chem 28:849–857. doi:10.1021/jm00145a002
16. GRID 22c (2004) Molecular Discovery Ltd. http://www.moldiscovery.com. Accessed 20 May 2014
17. Pentacle 1.0.6 (2010) Molecular Discovery Ltd. http://www.moldiscovery.com/. Accessed 20 May 2014

18. Durán A, Comesaña G, Pastor M (2008) Development and validation of AMANDA, a new algorithm for selecting highly relevant regions in molecular interaction fields. J Chem Inf Model 48:1813–1823. doi:10.1021/ci800037t
19. Mosmann T (1983) Rapid colorimetric assay for cellular growth and survival: application to proliferation and cytotoxicity assays. J Immunol Methods 6:55–63
20. Ohno M, Abe TJ (1991) Rapid colorimetric assay for the quantification of leukemia inhibitory factor (LIF) and interleukin-6 (IL-6). J Immunol Methods 145:199–203
21. Clothier RH (1995) The FRAME cytotoxicity test. Methods Mol Biol 43:109–118
22. Hawkins PCD, Skillman AG, Warren GL, Ellingson BA, Stahl MT (2010) Conformer generation with OMEGA: algorithm and validation using high quality structures from the Protein Databank and Cambridge Structural Database. J Chem Inf Model 50:572–584. doi:10.1021/ci100031x
23. Hawkins PCD, Nicholls A (2012) Conformer generation with OMEGA: learning from the data set and the analysis of failures. J Chem Inf Model 52:2919–2936. doi:10.1021/ci300314k
24. OMEGA 2.5.1.4 (2013) OpenEye Scientific Software, Santa Fe, NM. http://www.eyesopen.com. Accessed 20 May 2014
25. Halgren TA (1999) MMFF VII. Characterization of MMFF94, MMFF94s and other widely available force fields for conformational energies and for intermolecular interaction energies and geometries. J Comput Chem 20:730–748. doi:10.1002/(SICI)1096-987X
26. Gaillard P, Carrupt PA, Testa B, Boudon A (1994) Molecular lipophilicity potential, a tool in 3D QSAR: method and applications. J Comput Aided Mol Des 8:83–96
27. Pedretti A, Villa L, Vistoli G (2004) Vega—an open platform to develop chemo-bio-informatics applications, using plug-in architecture and script programming. J Comput Aided Mol Des 18:167–173